# Linking horizontal and vertical transports of biomass fire emissions to the Tropical Atlantic Ozone Paradox during the Northern Hemisphere winter season: II. 1998-1999

Gregory S. Jenkins[1]

Jung-Hee Ryu[1]

Anne M. Thompson[2]

Jacquelyn C. Witte [2]

[1]*Department of Meteorology, Pennsylvania State University*

[2] *SSAI at NASA Goddard Space Flight*

2/10/02

**Corresponding Address:**

Gregory S. Jenkins

503 Walker Building

University Park, PA 16802

e-mail: osei@essc.psu.edu

**Abstract**

The horizontal and vertical transport of biomass fire emissions in West Africa during November 1998 through February 1999, are examined using all available data including wind, fire, aerosol, precipitation, lightning and outgoing longwave radiation. Ozonesonde data from the Aerosols99 Trans-Atlantic cruise are also included with rain and wind analyses. The results here support earlier studies that ozone and ozone precursors associated with biomass burning are confined to the lower troposphere primarily due to the lack of deep convection over land areas. Ozone and its precursors are horizontally transported equatorward or towards the west by winds in the 1000-700 hPa layers. However, rising adiabatic motions associated with the diurnal evolution of the West African planetary boundary layer can transport ozone and its precursors vertically into the free troposphere above the marine boundary layer. Moreover, lightning from South America, Central Africa and mesoscale convective systems in the Gulf of Guinea can lead to elevated ozone mixing ratios in the middle and upper troposphere.

## 1. Introduction

During the Northern Hemisphere winter season biomass burning is found in the Northern Hemisphere north of the rainforest (~5-15°N) [Grégoire et al., 1999]. Satellite estimates [Fishman et al. 1991] and ship measurements, however, show lower values of tropospheric ozone over the north tropical Atlantic just downstream of fires relative to the south Tropical Atlantic therefore denoted as the "Ozone Paradox" [Thompson et al., 2000]. Based on the work of Thompson et al. [2000], relatively high ozone mixing ratios were confined to altitudes less than 5 km in the north tropical Atlantic and to the layer between 5km and 15km in the south tropical Atlantic. They attribute this pattern to biomass burning north of the Equator and a combination of inter-hemispheric transport, aged stratospheric –upper tropospheric ozone and ozone supplied by lightning nitric oxide.

Using climatological data for West Africa, Jenkins and Ryu [2002] found the following: (1) Fire counts and Aerosol indices had their highest values typically during January and February. (2) Winds at 925, 700 and 500 hPa had an easterly component in the regions where biomass burning occurs but were westerly at 200 hPa during the Northern Hemisphere winter. (3) At 700 hPa a persistent anticyclone was found between 10-15°N near the coastline of West Africa. (4) The areas of highest rain rates and lowest outgoing longwave radiation fluxes occurred over the central Atlantic away from land areas. Consequently, air was transported above the marine boundary layer by adiabatic lifting when air from land areas of West Africa is transported westward or equatorward. (5) While there was some evidence of lightning over West Africa, these values were small relative to South America and Central Africa. These results support the ozone paradox with relatively high ozone mixing ratios confined to the lower troposphere just downstream of West African fires due to the lack of deep convection. Over the south tropical Atlantic, the middle/upper troposphere is enriched with ozone by lightning transported from South America and Central Africa through a Walker-type circulation.

During the time period of January 21st through February 14th, surface ship measurements and ozone soundings were conducted [Thompson et al. 2000; Bates et al. 2001]. The ship's transect began at Norfolk VA (37°N, 76°W) and ended at Cape Town, South Africa (34°S, 22°E). Ozonesondes were launched each day at approximately 1200 UTC. We examine further the ozone vertical profiles and the associated tropical curculation during the period of January 23rd through January 28th when the ship made its closest approach to West Africa and biomass burning is widespread.

Figure 1 shows the 6 ozonesondes for the January 23rd through January 28th timeframe. As defined by Thompson et al. [2000], all of the ozonesondes except the last one fall in zone 2 (14°N-0). This zone is characterized by relatively high ozone in the 0-5 km range while in zone 3 (0-23°S) there is more ozone in the 5-10 km altitude range [Thompson et al. 2000]. This pattern is generally followed except that there are multiple peaks of higher ozone values in the lower, middle and upper troposphere on day 1 (Figure 1a) and two broad peaks on days 3, 4, and 5 (Figures 1 c-e) in the lower and middle troposphere. In profiles that have two ozone peaks, the peaks tend to occur between 2-3 km and near 8 km. The lower troposphere peaks are likely associated with biomass burning while lightning is most likely associated with higher values in the middle troposphere [Thompson et al. 2000].

Bates et al. [2001] identified the meteorological regimes during the AEROSOLS99 ship cruise for zones 2 and 3. In the latitudinal band of 15.5°N-8°N there was anticyclonic flow associated with the Azores high, which brought aerosols having a chemical signature of mineral dusts. In this zone, Figure 1 shows elevated ozone mixing ratios (55-75 ppbv) in the 1-5 km altitude range. As the ship moved in the latitudinal band of 8°N-3°N, wind direction shifted from the northeaster to southeaster with aerosols having a chemical signature of mineral dust and biomass burning. Figure 1d shows that the highest lower tropospheric value of ozone (80-90 ppbv) at 5.5°N in this zone. In the latitudinal band of 3°N-5°S southeasterly winds increased in speed and aerosols had a chemical signature associated with biomass burning. Figure 1e shows elevated ozone mixing ratio at approximately 3 km in agreement with back trajectory analysis by Voss et al. [2001]. At 2.2°S, the highest ozone mixing ratios are found at altitudes above 5 km, and is most likely due to lightning [Thompson et al. 2000].

The purpose of this paper is to examine the winter season circulation during 1998-1999 in order to determine both horizontal and vertical transport processes that would be associated with ozone or ozone precursors from biomass burning in West Africa. A second purpose is to examine the properties of the atmosphere associated with the vertical and horizontal transport of ozone and ozone precursors during the period of January 23rd through January 28th in order to understand the daily ozone profiles in the AEROSOLS99 Ship campaign.

## 2. Data Description

The NCEP reanalysis [Kalnay et al. 1996] averaged for November 1998- February 1999 and January 23rd-January 28th 1999 are used at horizontal resolution of $2.5° \times 2.5°$. The 1998-1999 monthly fire count data is produced from the Along Tracking Scanning Radiometer (ATSR) instrument which has a horizontal resolution of 1 km and a swath width of 512 km. Fires are identified at a fixed threshold of 312°K [Arino and Melinotte, 1995]. The monthly 1998-1999 and January 23rd-January 28th aerosol indices are produced on a $1° \times 1.25°$, but December 1998 is missing because fewer than 20 days were available to form a monthly average [Herman et al., 1997; Torres et al. 1998].

Rain estimates during the period of November-March 1998-1999 come from the TRMM Precipitation Radar (TRMM PR) at 2 km above the surface on a high-resolution ($0.5° \times 0.5°$) grid (denoted as TPRH) [Kummerow et al. 2001] and the TRMM Merged rain product [Adler et al., 2000]. Unconditional rain, convective and stratiform rain rates along with stratiform and convective mean storm heights are presented from the TRMM PR [Jenkins, 2000]. TRMM daily Rain estimate are computed from satellite derived and rain-gauge estimates for the period of January 23rd to January 28th on a $1° \times 1°$ grid [Huffman et al. 2001]. Monthly merged rain estimates (CMAP) for 1998 and 1999 are produced on a 2.5° × 2.5° grid [Xie and Arkin, 1997]. Ozonesonde data for the Aerosols99 ship campaign was obtained from the SHADOZ website [Thompson et al. 2000; Thompson et al. 2002]

## 3. Results

### 3.1 1998-1999 monthly averaged circulation and precipitation

Figures 2a and b show the geographic distribution of monthly fire and aerosol indices during January 1999. Fires were located in the latitudinal range of 5°N and 15°N and extended from the coastline eastward to 35°E. High value of aerosol indices (>1.4) are found to the west and south of the region of the biomass burning which is the downstream of fires. For the time period of October 1998 through March 1999, the highest fire counts and aerosol index values are found during January 1999. This highly correlated pattern is consistent with the results from Jenkins and Ryu [2002] and Goloub and Arino [2000]. Figures 3 through 6 shows the 925, 700, 500 and 200 hPa zonal winds and streamlines for November 1998 through February 1999. At the lowest altitudes (925 hPa) northeasterly and southeasterly winds converge near 5°N with the general flow directed out towards the Atlantic Ocean (Figures 3a, 4a, 5a, 6a). Stronger easterly and northeasterly winds are found over the ocean areas away from the West African coastline. Hence, rising plumes of air from biomass burning would be transported towards the Atlantic Ocean in the absence of moist convective processes.

At 700 hPa, strong easterly winds just equatorward of an anticyclone is found to persist from November 1998 through February (Figures 3b, 4b, 5b, 6b). This feature was also found for averaged 1979-1992 period [Jenkins and Ryu, 2002]. A large zone of easterly winds with speeds greater than 8 m/sec can be found in extreme southern sectors of West Africa, while the core of strongest winds (> 12 m/sec) is found over the ocean. Thus, ozone or its precursors that are vertically transported to this pressure level would be rapidly transported westward over the

Atlantic Ocean. At 500 hPa an anticyclone is centered between 5-15°N and easterly winds are found equatorward of the anticyclone's axis (Figures 3c, 4c, 5c and 6c). Zonal winds at this pressure level are weaker than those found at 700 hPa. At the 200 hPa level, westerly winds are found throughout most of the tropical Atlantic, except for ocean areas adjacent to Central Africa (Figures 3d, 4d, 5d, 6d) during January and February 1999.

Figures 7a-d show the November 1998 through February 1999 OLR fluxes. During November and December the lowest OLR values are found over the central Atlantic near 30°W, while during January and February the pattern of low OLR values are nearly zonal. The OLR values over the tropical Atlantic during January and February are somewhat lower than the climatological values reported by Jenkins and Ryu [2001] and suggestive of deeper convection. The highest CMAP precipitation rates are generally found over the Atlantic between the longitudes of 40°W-20°W and the latitudes of the Equator to 10°N (Figures 8a-d). During February 1999, relatively high rain rates are found over southern areas of Nigeria (5°N, 10°E) and could serve as a site for vertical transport of ozone and its precursor from the PBL into the free troposphere.

Figures 9 shows a vertical cross-section of TRMM PR unconditional rain rates at 10°W during January and February 1999 (Figures 9a, b). We find the highest rain rates at altitudes lower than 5 km and mainly confined to latitudes near the Equator and in the Southern Hemisphere. The TRMM PR and TRMM Merged rain rates are approximately 4-5 mm/day over the ocean areas just equatorward of the West African coastline (2°S-5°N, 25°W-10°E) during November 1998 through March 1999 (Figure 9c). Convective and stratiform rain occurs in this region with the convective rain producing most of the rain (Figure 10a). Convective rain accounts for more than 65% of the total rain, while stratiform rain accounts for 25-35% of the rain during 1998 and 1999 (Figure 10b).

The mean convective storm heights (height with the minimum detectable reflectivity –17 DBZ) and mean stratiform storm heights (level of the melting layer) are generally between 5 and

6 km from November through February during 1998-1999 (Figures 10c). These storm heights are consistent with relatively high OLR values and imply that the vertical transport of ozone and its precursors via convection would be confined to altitudes lower then 6 km. Higher mean convective and stratiform heights are found during March as 1998 as the region of heaviest rainfall moves poleward with the onset of Northern Hemisphere spring season.

## 3.2 CIRCULATION, OZONE, AEROSOLS,PRECIPITATION AND LIGHTNING DURING JANUARY 23$^{RD}$ – JANUARY 28$^{TH}$ 1999.

Examination of Figure 1 shows dual or multiple peaks in the ozone vertical profiles from January 23$^{rd}$ through January 28$^{th}$. Here, we link the horizontal and vertical transport processes to the ozone measurements with the hope of identifying the cause of these peaks in ozone mixing ratio.

### 3.2.1 Horizontal Circulation

Figure 11 shows the mean 11-day (January 18$^{th}$-28$^{th}$) wind fields at 925, 850, 700, 500, 300 and 200 hPa and the location of the ship from January 23$^{rd}$-28$^{th}$ The prevailing lower tropospheric winds during this period have an easterly component with a core of strong winds at 700 hPa just off the coast of West Africa. Anticyclonic flow is found in the middle/upper troposphere with easterly winds located to equatorward side and westerly winds located to the poleward side of the anticyclone (Figure 11d-f). Prevailing westerly winds are found north of the Equator at 200 hPa during the 11 day period.

Five-day back trajectories from the location of the ship shows good agreement with mean easterly winds in the lower troposphere (925, 850 and 700 hPa) (Figure12). At the lowest level, the air has its origins over northwest or western Africa during January 23$^{rd}$-26$^{th}$. After this time the origin of the air is less certain, but a likely source region is the Southern Tropical Atlantic. This may be related with the decrease of the ozone mixing ratio in the lower troposphere (Figure

1e and f). At 850 and 700 hPa, the origin of the air is either West Africa or just downstream of it. Consequently, ozone mixing ratios would be elevated at these levels relative to 925 hPa. Elevated ozone mixing ratios can be found below 5 km from January 23rd through January 28th [Figure 1].

The greatest variations in the back trajectory analysis are found in the middle/upper (500 and 300 hPa) troposphere (Figure 12). For example at 500 hPa, the North Tropical Atlantic is the origin of air during January 23rd- January 25th, while the South Tropical Atlantic is the source of the air from January 26th-January 28th. A similar degree of variability is also found at 300 hPa. We believe that the primary reason is due to northeastward propagating anticyclones in the middle/upper troposphere. Figures 13 and 14 shows the 500 and 300 hPa instantaneous flow at 1200 UTC and the approximate position of the ship. In each case, the ship passed through the poleward and equatorward sides of the anticyclone. Moreover, the anticyclones had their origins near South America.

### 3.2.2 Ozone mixing ratios and Aerosols

The ozone mixing ratios averaged over various pressure levels in the lower, middle and upper troposphere are shown in Figures 15 a-c. In the lower troposphere the highest ozone mixing ratios are found in the 850-700 hPa layer each day. An average ozone mixing ratio of 52 ppbv is found during the 6 days in the 850-700 hPa layer compared to 31 and 37 ppbv in the surface-925 hPa and 925-850 hPa layers, respectively (Figure 15a). The ozone mixing ratio of the lower troposphere (especially from the surface to 850 hPa) is relatively high from January 25th-27th when the ship is located downstream of biomass burning over West Africa but undergoes a significant decrease on January 28th in association with a wind direction change from northeasterly to southeasterly. In the middle troposphere higher average ozone mixing ratios tend to occur during January 26th through January 28th. In January 28th relatively high ozone mixing ratios are found at altitudes above 600 hPa. The middle troposphere average ozone mixing ratios vary between 52 and 56 ppbv during the 6 days with the highest value of 56 ppbv found in the 500-400 hPa layer (Figure 15b). In the upper troposphere, the highest ozone mixing ratios are found in the 400-300 hPa layer. In this layer, there is an increase in the second portion of the period, with values approaching 84 ppbv on January 28$^{th}$ (Figure 15c). We believe that the high values on January 28$^{th}$ are associated with MCSs just off the coast of West Africa, which produced lightning (see below) and may also have vertically transported ozone and ozone precursors from areas of biomass burning into the middle/upper troposphere. The ozone mixing ratio averaged in the upper troposphere has a range of 44-52 ppbv with the highest values in the 400-300 hPa layer.

Figures 16 a-f shows the daily aerosol index over West Africa and the Tropical Atlantic Ocean. On January 23$^{rd}$ through January 24$^{th}$, high aerosol indices are found primarily over land areas, extending just offshore into the Gulf of Guinea (Figs. 16a, b). However, beginning on January 25$^{th}$ and running through January 28$^{th}$, a westward propagation of higher aerosol indices are found (Figures 16c-f). The ship is on the western boundary of this westward propagating area of high aerosol indices and therefore may miss the highest aerosol index values. These aerosols are being carried westward by easterly winds in the lower or middle troposphere. The aerosols are produced through biomass burning and therefore associated with ozone. Consequently, the horizontal transport of aerosols is probably occurring in the 850-700 hPa layer where the highest ozone mixing ratios are found (Figure 15).

### 3.2.3 Precipitation, Vertical motions and Lightning

Daily precipitation rates as estimated from satellites show precipitation near the location of the ship during January 26$^{th}$-January 28$^{th}$ (Figure 17). Over land areas there little or no precipitation is found during this period. Consequently, the vertical transport of ozone or itsprecursors is unlikely through convective processes over land.

The lack of convection over West Africa, leads to the conclusion that vertical transport of ozone and its precursors most likely occurs through adiabatic lifting. The marine boundary layer (MBL) depth of 0.5 and 2 km is estimated through virtual potential temperature ($\theta_v$) from ship measurements (Figure 18). This value differs from Bates et al. (2001) who suggested a well mixed MBL up to 7 km using relative humidity the measure of MBL depth. We believe that $\theta_v$ provides a better estimate of MBL depth because RH is a function of temperature. Consequently, near saturated atmospheric conditions (as estimated from RH) do not necessarily imply significant vertical mixing as air temperatures are also varying with height. Moreover, the height of MBL does not undergo significant diurnal variations because of the ocean's large thermal heat capacity. Land areas over West Africa have a deeper PBL depth and undergo significant variations in depth because of the low thermal heat capacity of land. The NCEP reanalysis data suggests that the PBL reaches its greatest depths between 1200 and 1800 UTC. The estimated depth of the PBL over West Africa is 2-3 km. Contours of north-south and east-west vertical cross sections of potential temperature for January, February 1999 are consistent with the work of Jonquieres et al. [1998] which show that parcels of air over land areas of West Africa would flow above the marine boundary layer through adiabatic motion (Figure 19).

The production of ozone (4-8 ppbv per day) as a result of lightning in Central Africa has been suggested by Thompson et al.[2000]. A large number of lightning flashes as detected by the LIS instrument are found near the continental outflow regions of both South American and Central Africa from December 1998 through March 1999 (Figure 20a). Central Africa has a larger number of lightning flashes (> 10000 flashes per month) but the prevailing winds are westerly making South America a more likely candidate for high ozone mixing ratios above 300 hPa. Ozone mixing ratios in the middle troposphere during January 1999 and during the Aerosols99 campaign are likely enhanced by lightning in Central Africa since the prevailing winds are easterly.

During the period of January 20th through January 31st an average of 354 lightning flashes per day (Figure 20b) occurred in continental outflow regions of South America (0-20°S, 56°W-36°W). An average of 543 flashes per day occurred in continental outflow regions of Central Africa (4°N-16°S, 9°E-29°E). Near the end of January, the number of lightning flashes in Central Africa significantly larger than that in South America. Moreover, the rain cluster located off the coast of West Africa was associated with the lightning (61 flashes detected by LIS) during the morning of January 27th. From the streamline distribution of the middle and upper troposphere (Figure 13 and 14), we can suggest that the increase of the ozone mixing ratio in the middle troposphere (8~10km) is associated with the lightning from the rain cluster located off the coast of West Africa while the increase in the upper troposphere (~13km) comes from the lightning over the South America. However, the trajectory analysis as well as the distribution of the streamline do not support lightning on January 27th as the origin of high ozone mixing on January 28th. But the middle and upper troposphere trajectory analysis may in error due to an anticyclone near the MCSs which may have circulated lightning produced ozone near the vicinity of the ship.

Consequently, the lack of precipitation during this period over West Africa suggests that the vertical transport of ozone, aerosols and ozone precursors into the free troposphere can be occurring through adiabatic lifting or vertical mixing during the afternoon hours when the PBL height reaches its highest values. The exception is in the Gulf of Guinea on January 27th where an MCS associated with lightning and presumably strong updrafts occurred.

## 4. Conclusion

In this paper, we have examined on Northern Hemisphere winter circulation in the context of a ship measurement campaign that took place in late January and early February of

1999. In particular we have focused on the 6 days between January 23rd and January 28th 1999. Our findings are:

- The fire count and aerosol index in West Africa had its highest values during January 1999. Moreover, fires were located the latitude range of 5-15°N.
- During November 1998 through February 1999 there is northeasterly or easterly winds over the tropical Atlantic Ocean in the lower troposphere from 925 hPa through 500 hPa. The time-averaged winds from November through February show a quasi-stationary anticyclone at 700 and 500 hPa with strong zonal winds at 700 hPa being associated with the anticyclone. At pressure levels less than 300 hPa, the winds are westerly throughout much of the Atlantic except for regions in the Southern Hemisphere near Central Africa.
- The lowest OLR values and the highest rain rates are found over the Central Atlantic. Over the land areas in West Africa, OLR values of 260-280 $W\text{-}m^{-2}$ are found implying that deep convection was rarely found from November 1998 through February 1999. The meteorological properties from November 1998 through February 1999 are consistent with the climatological results from Jenkins and Ryu [2002].
- The TRMM data shows that while convective rain is responsible for most of the rain in areas south of the West African coastline, the mean convective storm heights were approximately 5-6 km again suggesting the lack of deep convection. Lightning was found over the Central Africa and the South America during January 1999.
- During the January 23-27th, easterly winds in the lower troposphere from areas of biomass burning in West Africa appears to be responsible for the peak in ozone mixing ratios in the 2-4 km altitude range. The vertical transport of ozone to the lower troposphere is most likely associated with adiabatic lifting of westward or equatorward moving air-mass from biomass burning regions. Because of the lack of deep convection over West Africa, biomass burning is not responsible for elevated ozone mixing ratios in the middle and upper troposphere. Rather, lightning and the subsequent production of

ozone from Central Africa or South American and then horizontal transport are responsible for elevated ozone mixing ratios in the middle/upper troposphere.

- A transition in the circulation during Jan. 23rd-Jan. 28th occurs near 2.2°N at 925 and 850 hPa. In this case, the air parcels have their origins over the South Atlantic Ocean leading to lower ozone mixing ratios. At 700 hPa, the winds are easterly and air parcels still have their source region in West Africa near biomass burning. In the upper troposphere, northeastward moving anticyclones complicate horizontal transports of air, which produces uncertainty in the 5 day trajectory analysis.
- The high ozone mixing ratios on January 28th are due to lightning and the venting of ozone and ozone precursors from the lower troposphere in association with an MCS just off the coast of West Africa on January 27th and possibly ozone production through lightning in South America.

Overall, the results suggest that biomass burning is an important contributor to ozone primarily in the lower troposphere of the Northern Hemisphere from November through February. The lack of deep convection during this period limits the vertical transport of ozone and its precursors into the upper troposphere. Consequently, ozone destruction through photolysis and deposition is probably significant in the PBL in regions downstream of the fires in West Africa providing one part of the solution to the "ozone paradox" in West Africa. The horizontal transport of ozone towards the Americas by relatively strong easterly winds also limits the accumulation of ozone in the lower troposphere. It appears, however, that ozone is reaching the free troposphere as evidence of high mixing ratios at 850 and 700 hPa. Transport to the free troposphere occurs via adiabatic lifting of westward or equatorward moving air from West Africa above the MBL.

Based on the results presented here and the results of Jenkins and Ryu, [2002], the other solution to the ozone paradox, is that lightning directly enhances ozone mixing ratios in the middle/upper troposphere in the south tropical Atlantic during Northern hemisphere winter. In fact, lightning may be a more important ozone source than biomass burning especially in the continental outflow regions near Africa during Northern hemisphere autumn. Model simulations by Moxim and Levy [2000] suggests that the September, October, November ozone maximum may have occurred prior to the practice of biomass burning because of lightning. As their simulations show, lightning is responsible for high ozone mixing ratios in the upper troposphere. Moxim and Levy [2000] show that lightning enhances $O_3$ mixing ratios and NO mixing ratios in the middle/upper troposphere while biomass burning enhances $O_3$ and NO mixing ratios in the lower troposphere.

We believe that a field experiment with sampling over West Africa and the adjacent ocean areas will provide the evidence to support the results presented in this paper. Sampling the upper troposphere should link lightning from South America, Central Africa and Atlantic MCSs to elevated middle and upper troposphere ozone mixing ratios. In continental areas, high ozone mixing ratios and aerosol concentrations near the surface may be causing a significant health risk to inhabitants, especially the young and elderly in West Africa. Thus, monitoring sites in West Africa would help in understanding the health aspects of biomass burning and provide an estimate ozone destruction rates between West Africa and the adjacent Atlantic Ocean.

**Acknowledgements**

This research was supported through NSF Grant ATM-0105206 and NASA Grant NAG5-7443. Lightning data provided by the NASA Lightning Imaging Sensor (LIS) science team and the LIS data center located at the Global Hydrology and Climate Center (GHCC), Huntsville, Alabama

**References**

Adler, R. E., G. J. Huffman, D. T. Bolvin, S. Curtis, E. J. Nelkin, Tropical Rainfall Distributions determined using TRMM combined with other Satellite and Rain Gauge

Information, *J. Applied Meteorology,* **39**, 2007-2023, 2000.

Arino, O. and J-M. Melinotte, The Fire Atlas, Earth Observation Quarterly, 50, December 1995.

Bates, T. S., P. K. Quinn, D. J. Coffman, J. E. Johnson, T, L. Miller, D. S. Covert, A. Wiedensohler, S. Leinert, A. Nowak, and C. Neususs, Regional physical and chemical properties of the marine boundary layer aerosol across the Atlantic during Aerosols99:An overview, *JGR*, **106**, 20,767-20,782, 2001.

Fishman, J., K. Fakhruzzaman, B. Cros, D. Nganga, Identification of Widespread Pollution in the Southern Hemisphere Deduced from Satellite Analyses, *Science,* **252**, 1693-1696, 1991.

Grégoire, J-M., S. Pinnock, E. Dwyer, E. Janodet, 1999: Satellite monitoring of vegetation fires for EXPRESSO: Outline of activity and relative importance of the study area in the global picture of biomass burning, *JGR*, **104**, 30691-30699, 1999.

Goloub, P, and O. Arino, Verification of the consistency of POLDER Aerosol Index over land with ATSR-2/ERS-2 fire product, *GRL*, **27**, 899-902, 2000.

Herman, J.R., P.K. Bhartia, O.Torres, C. Hsu, C. Seftor, E. Celarier, Global Distribution of UV-Absorbing Aerosols From Nimbus-7/TOMS Data, JGR, 102, 16,911-1,922, 1997.

Huffman GJ, Adler RF, Morrissey MM, Bolvin DT, Curtis S, Joyce R, McGavock B, Susskind J, Global Precipitation at One-Degree Daily Resolution from Multisatellite Observations, *J. Hydrometeorology*, **2**, 36-50, 2001.

Jenkins, G. S., TRMM satellite estimates of convective processes in Central Africa during September, October, November 1998: Implications for elevated Atlantic tropospheric ozone, *GRL*, **27**, 1711-1714, 2000.

Jenkins, G. S., and J-H. Ryu, Linking horizontal and vertical transports of biomass fire emissions to the Tropical Atlantic Ozone Paradox during the Northern Hemisphere winter season: I. Climatology, 2002 [This issue].

Kalnay, E., M. Kanamitsu, R. Kistler, W. Collins, D. Deaven, L. Gandin, M. Iredell, S. Saha, G. White, J. Woollen, Y. Zhu, A. Leetmaa, B. Reynolds, M. Chelliah, W. Ebisuzaki, W.

Higgins, J. Janowiak, K.C. Mo, C. Ropelewski, J. Wang, Roy Jenne, Dennis Joseph, The NCEP/NCAR 40-Year Reanalysis Project. *Bulletin of the American Meteorological Society*: Vol. **77**, No. 3, pp. 437-472, 1996.

Kummerow, C., W. Barnes, T. Kozu, J. Shieu, J. Simpson, The Tropical Rainfall Measuring Mission (TRMM) Sensor Package, *J. Atmospheric and Oceanic Technology,* **15**, 809-817, 1998.

Moxim, W. J., and H. Levy II, A model analysis of the tropical South Atlantic Ocean tropospheric ozone maximum: The interaction of transport and chemistry, *JGR*, **105**, 17,393-17,415, 2000.

Thompson, A. M. et al., A Tropical Atlantic Paradox: Shipboard and Satellite Views of a Tropospheric Ozone Maximum and Wave-one in January-February 1999, *GRL,* **27**, 3317-3320, 2000.

Thompson, A.M., J.C. Witte, R.D. McPeters, S.J. Oltmans, F.J. Schmidlin, J.A. Logan, M.Fujiwara, V.W.J.H. Kirchhoff, F. Posny, G. J.R. Coetzee, B. Hoegger, S. Kawakami, T. Ogawa, B.J. Johnson, H. Vömel and G. Labow, The 1998-2000 SHADOZ (Southern Hemisphere Additional Ozonesondes) Tropical Ozone Climatology. 1. Comparisons with TOMS and Ground-based Measurements, *JGR* - Atmospheres, in press, 2002.

Torres, O., P.K. Bhartia, J.R. Herman, Z. Ahmad, and J. Gleason, Derivation of aerosol properties from satellite measurements of backscattered ultraviolet radiation: Theoretical basis, *JGR,* **103**, 17099-17110, 1998.

Voss, K. J., E. J. Welton, J. E. Johnson, M. Thompson, P. K. Quinn, and H. Gordon, Lidar measurements during Aerosol99, *JGR*, **106**, 2001.

Xie, P. and P. A. Arkin, 1997. Global Precipitation: 17 -Year Monthly Analysis Based on Gauge Observations, Satellites Estimates and Numerical Model Outputs, *BAMS,* **78**, 2539-2558.

**FIGURE CAPTIONS**

**Figure 1.** Ozonezonde profiles launched during the Ship Campaign. (a) 1/23; (b) 1/24; (c) 1/25; (d) 1/26; (e) 1/27; (f) 1/28. Vertical axis is altitude in km, horizontal axis represents ozone mixing ratio in units of ppbv.

**Figure 2.** (a) January 1999 geographic distribution of Fires in West Africa. (b) January 1999 West African aerosol indices.

**Figure 3.** November 1998 Zonal wind speeds and wind streamlines. (a) 925 hPa; (b) 700 hPa; (c) 500 hPa; 200 hPa. Units are m/sec. Easterly winds < -4 m/sec are shaded, darkest shading corresponds to winds <-12 m/sec.

**Figure 4.** Same as Figure 3 except for December 1998.

**Figure 5.** Same as Figure 3 except for January 1999.

**Figure 6.** Same as Figure 3 except for February 1999.

**Figure 7.** Outgoing longwave longwave radiation over Western Africa, the adjacent Tropical Atlantic. (a) November 1998; (b) December 1998; (c) January 1999; (d) February 1999. Units are $W\text{-}m^{-2}$. Contours are shaded for values less than 240 $W\text{-}m^{-2}$.

**Figure 8**. CMAP rain rates over Western Africa, the adjacent Tropical Atlantic. (a) November 1998; (b) December 1998; (c) January 1999; (d) February 1999. Units are $mm\text{-}day^{-1}$. Contours are shaded for values greater than 4 $mm\text{-}day^{-1}$.

**Figure 9.** (a) January 1999 TRMM PR vertical cross-section of unconditional rain rates at 10°W; (b) February 1999 TRMM PR vertical cross-section of unconditional rain rates at 10°W; (c) Nov. 1998- March 1999 TRMM PR and TRMM Merged rain rates averaged over (2°S-5°N, 25°W-10°E). Units are $mm\text{-}day^{-1}$.

**Figure 10**. (a) Nov. 1998- March 1999 TRMM PR Convective and Stratiform Rain Rates for (2°S-5°N, 25°W-10°E); (b) Nov. 1998- March 1999 TRMM PR Convective and Stratiform rain

fraction for (2°S-5°N, 25°W-10°E); (c) Nov. 1998- March 1999 TRMM PR Convective and Stratiform mean storm heights for (2°S-5°N, 25°W-10°E); Units for rain rates are mm-day$^{-1}$, units for storm heights are meters.

**Figure 11.** January 18-28$^{th}$ time averaged zonal winds and streamline. (a) 925 hPa, (b) 850 hPa, (c) 700 hPa, (d) 500 hPa, (e) 300 hPa, (f) 200 hPa. Units are m/sec. Easterly winds < -4 m/sec are shaded, darkest shading corresponds to winds <-12 m/sec. The ship locations for the period of January 23-28$^{th}$ are represented by a black circle.

**Figure 12.** Five day Kinematic back trajectory analysis at 925, 800, 700, 500 and 300 hPa. (a) 1/23, (b) 1/24, (c) 1/25. (d) 1/26, (e) 1/27, (f) 1/28.

**Figure 13.** 500 hPa Zonal wind speeds and wind streamlines. (a) 1/23, (b) 1/24, (c) 1/25. (d) 1/26, (e) 1/27, (f) 1/28. Units are m/sec. Easterly winds < -4 m/sec are shaded, darkest shading corresponds to winds <-12 m/sec. The ship locations for the period of January 23-28$^{th}$ are represented by a black circle. Same as Figure 11 except for 700 hPa.

**Figure 14.** Same as Figure 13 except for 300 hPa

**Figure 15.** Ozone mixing ratios from the ozonesonde launches at various pressure levels from 1/23/99-1/28/99. (a) lower troposphere; (b) middle troposphere; (c) upper troposphere. Units are ppbv.

**Figure 16.** Daily Aerosol Indices over West Africa and the Tropical Atlantic. (a) 1/23; (b) 1/24; (c) 1/25; (d) 1/26; (e) 1/27; (f) 1/28. The ship locations at the time of the ozonesonde launch are represented by a black.

**Figure 17.** Daily rain rates over the Tropical Atlantic. (a) 1/23; (b) 1/24; (c) 1/25; (d) 1/26; (e)1/27; (f) 1/28. Units are mm-day$^{-1}$. The ship location at the time of the ozonesonde launch is represented by a black.

**Figure 18.** Daily profiles of the virtual potential temperature during the Ship Campaign. (a) 1/23; (b) 1/24; (c) 1/25; (d) 1/26; (e) 1/27; (f) 1/28.

**Figure 19.** NCEP 1000-600 hPa vertical cross-section of Potential Temperatures at 10°W. (a) January 1999; (b) February 1999. Units are degree K.

**Figure 20.** Detected lightning flashes over South American and Central African Outflow regions. (a) Monthly total flashes; (b) January 20-31 total flashes.

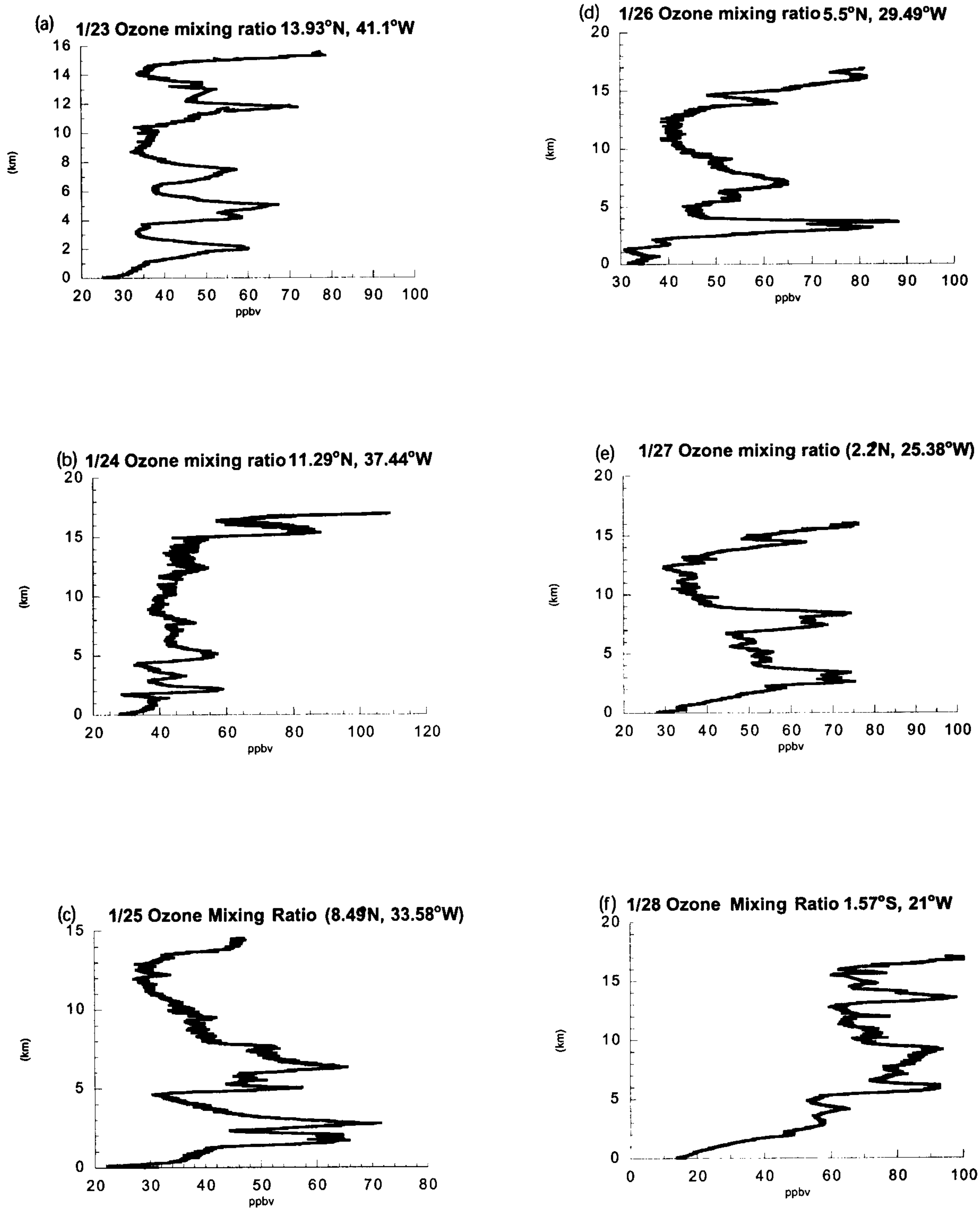
(a) 1/23 Ozone mixing ratio 13.93°N, 41.1°W
(km)
ppbv
(d) 1/26 Ozone mixing ratio 5.5°N, 29.49°W
(km)
ppbv
(b) 1/24 Ozone mixing ratio 11.29°N, 37.44°W
(km)
ppbv
(e) 1/27 Ozone mixing ratio (2.2N, 25.38°W)
(km)
ppbv
(c) 1/25 Ozone Mixing Ratio (8.49N, 33.58°W)
(km)
ppbv
(f) 1/28 Ozone Mixing Ratio 1.57°S, 21°W
(km)
ppbv

**Figure 1**

Month composite of ATSR fire counts : JAN. 99
1.5 X 1.5 degree

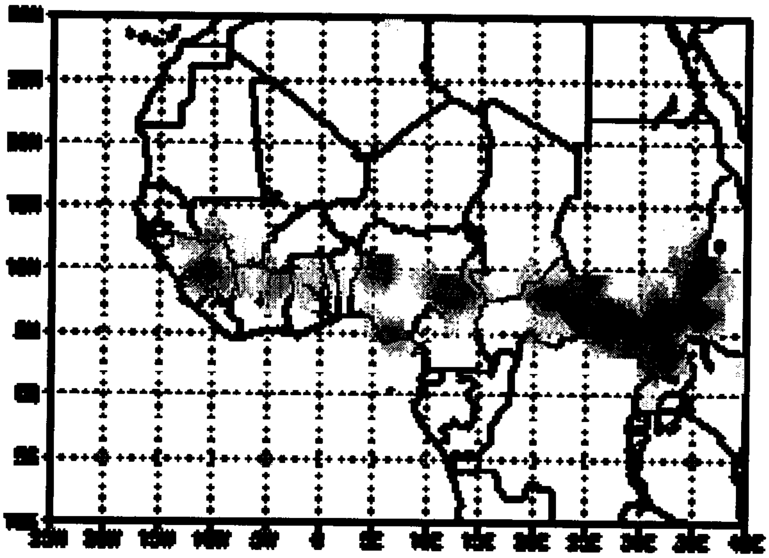

January 99 Aerosol Index

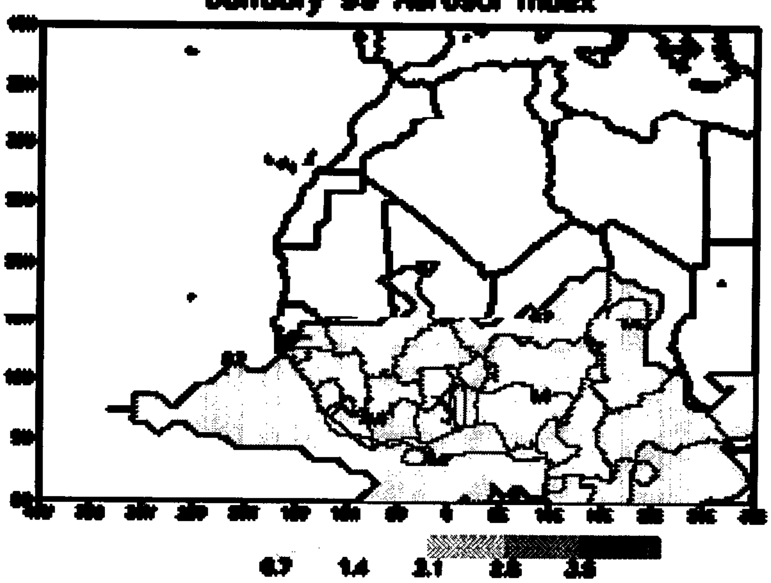


Figure 2

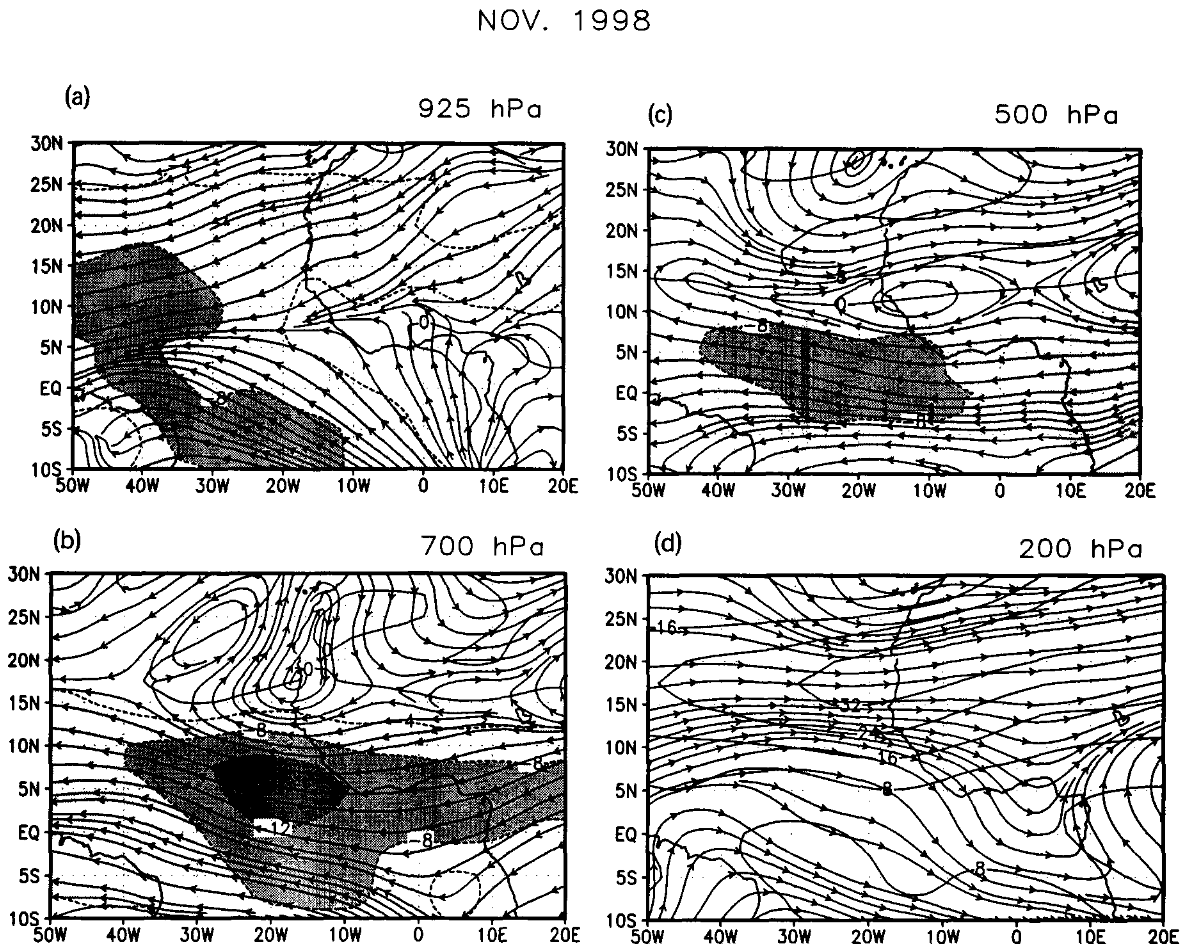


Figure 3

DEC. 1998

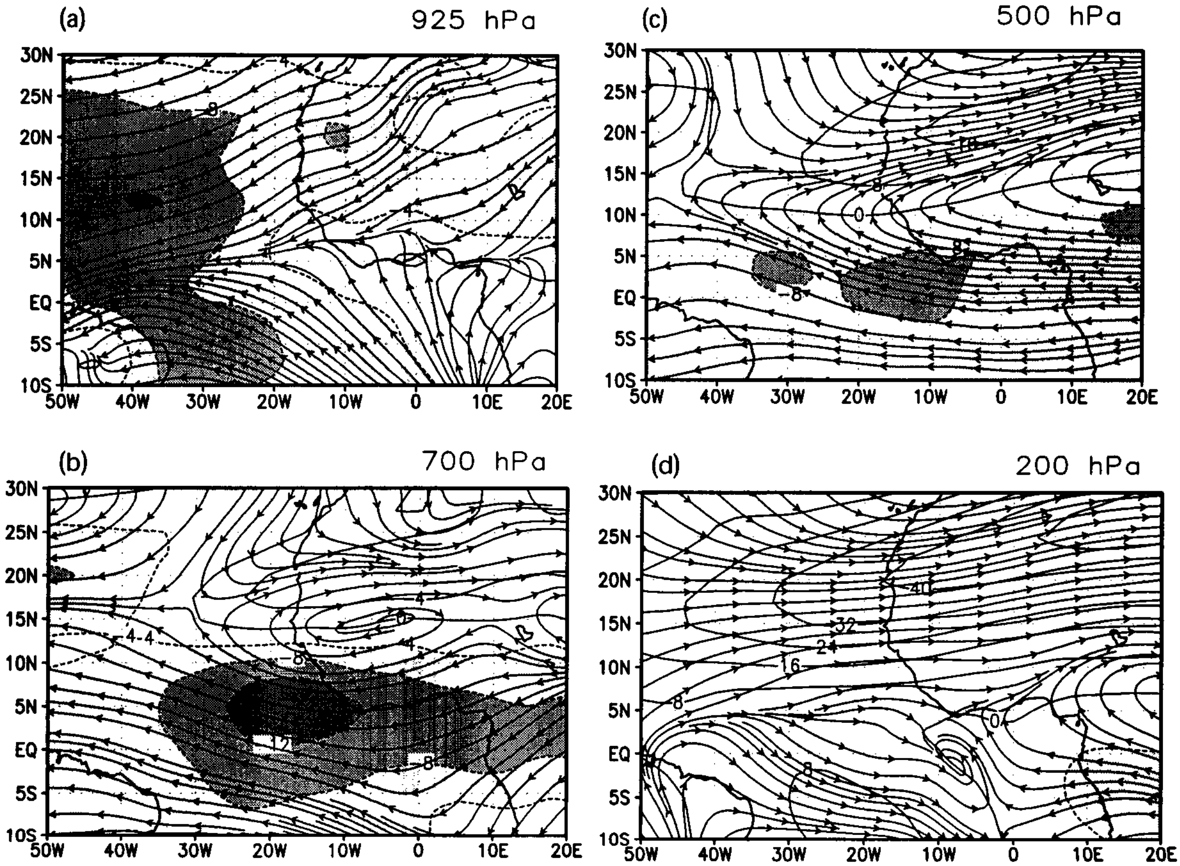


Figure 4

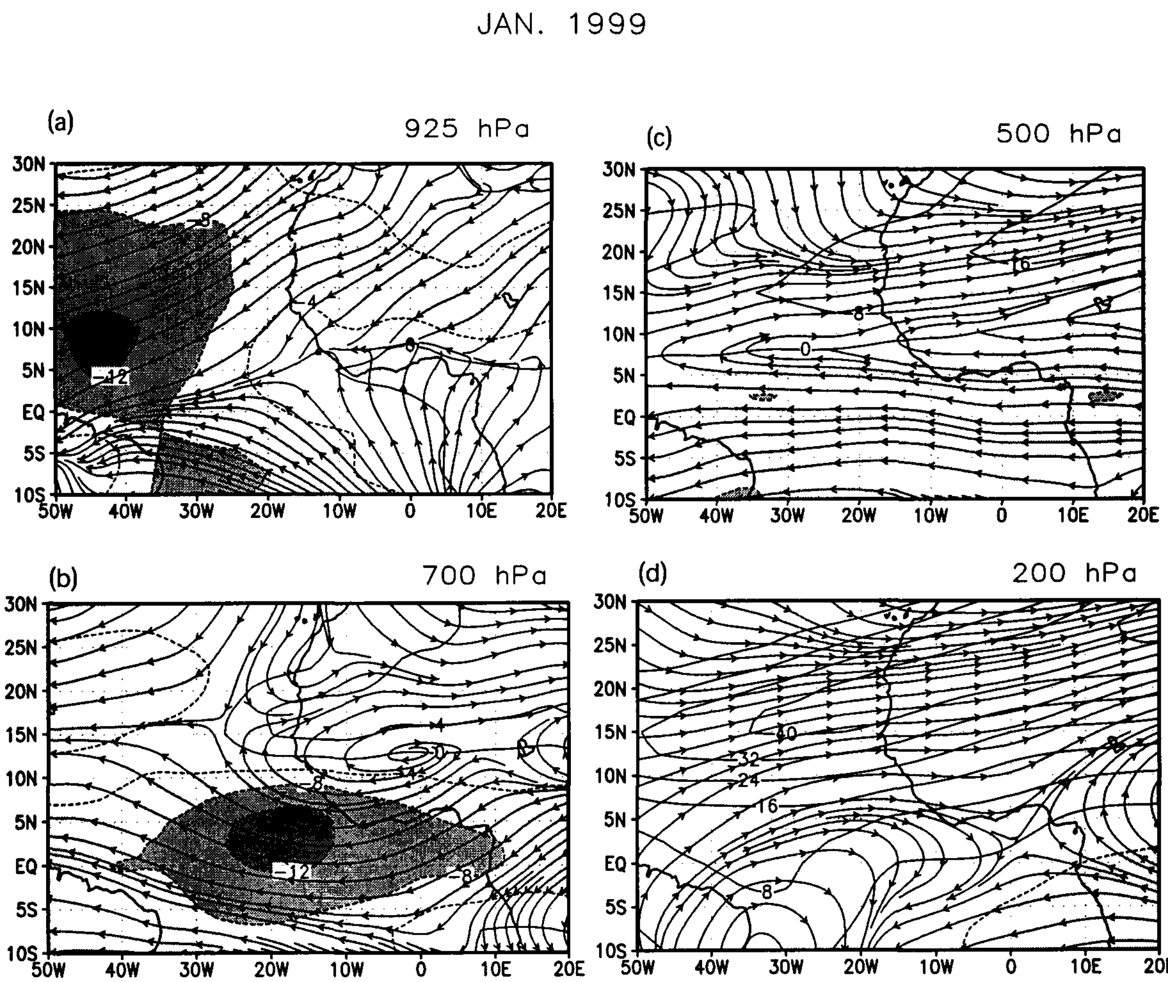
JAN. 1999
(a)
925 hPa
(c)
500 hPa
(b)
700 hPa
(d)
200 hPa
30N
25N
20N
15N
10N
5N
EQ
5S
10S
50W
40W
30W
20W
10W
0
10E
20E

Figure 5

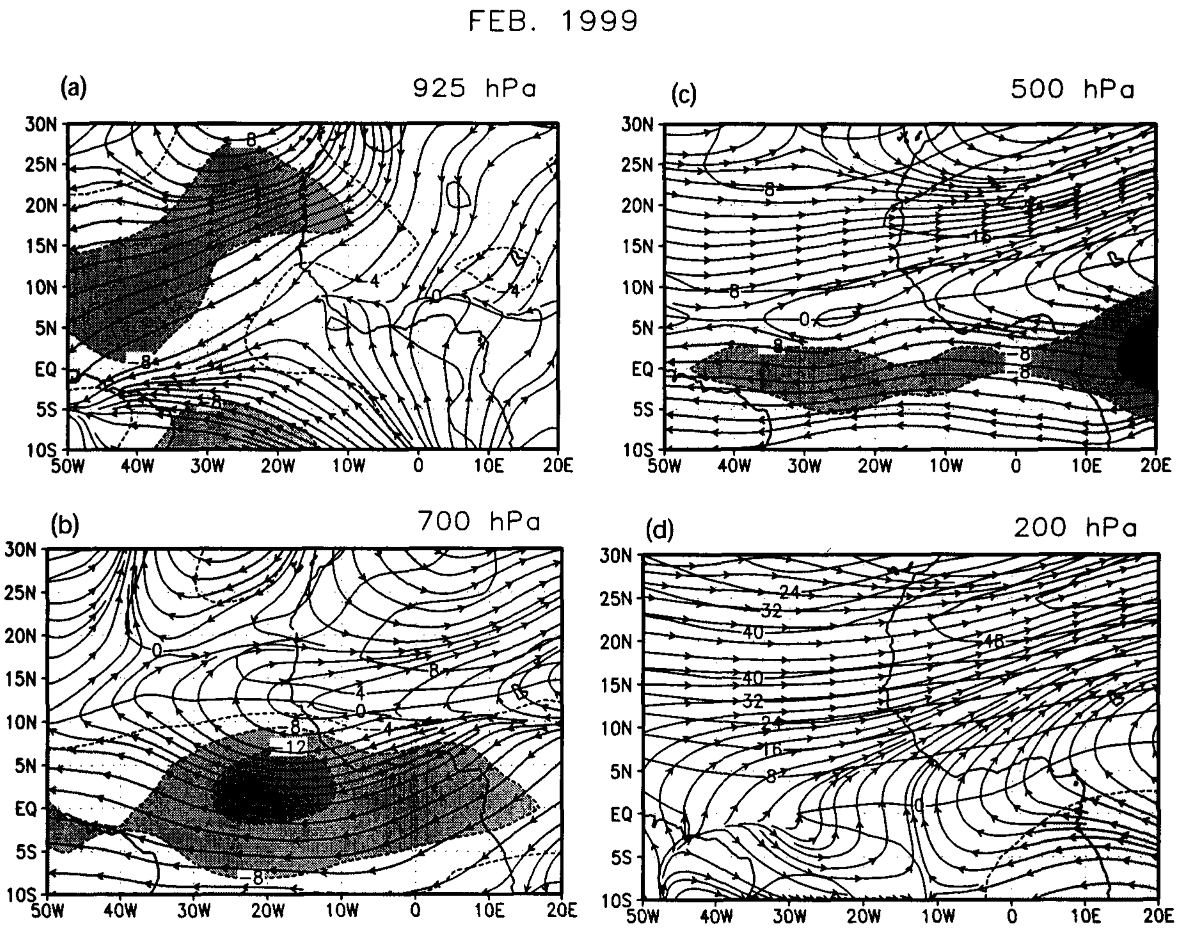


Figure 6

Outgoing Longwave Radiation

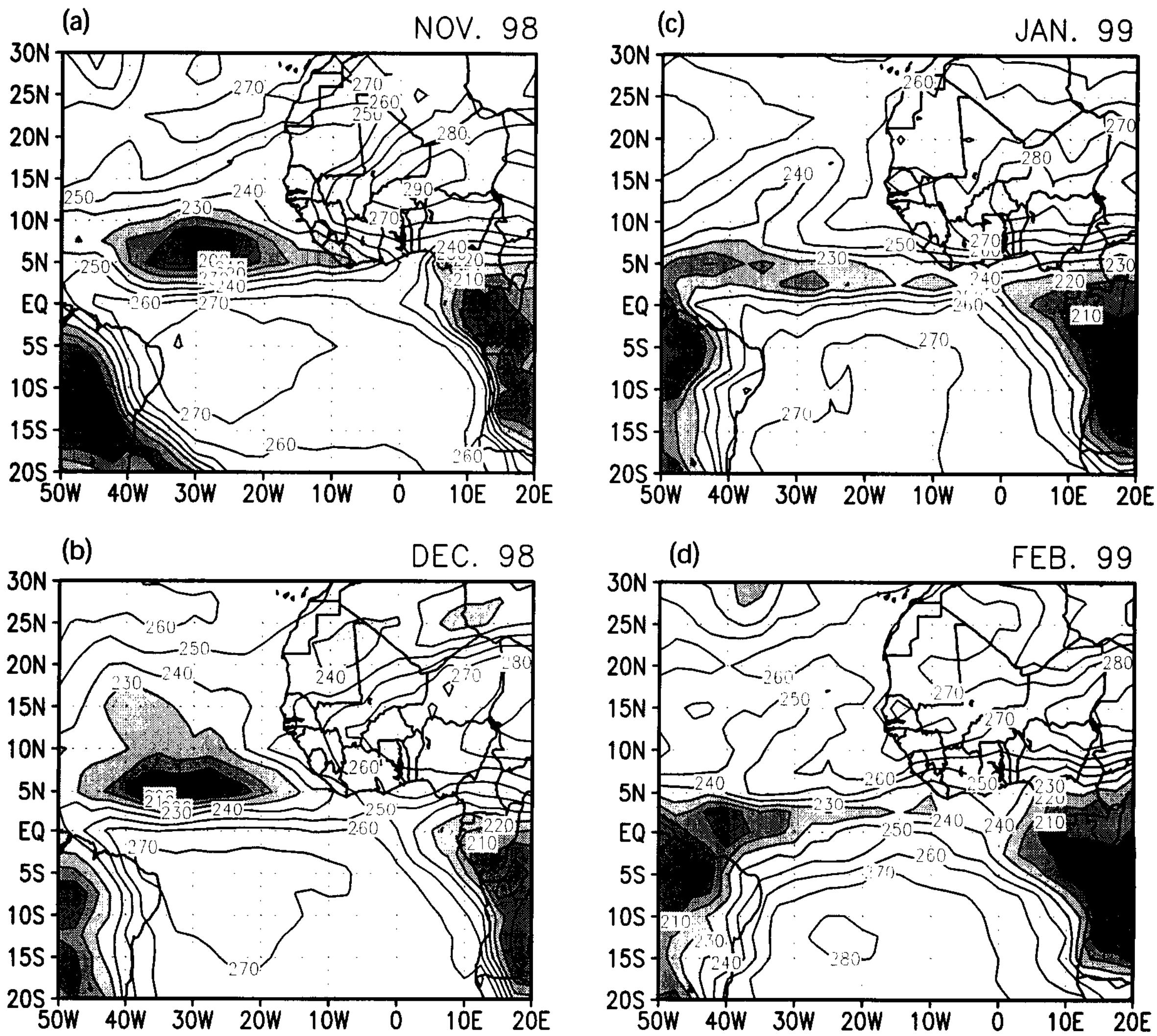


Figure 7

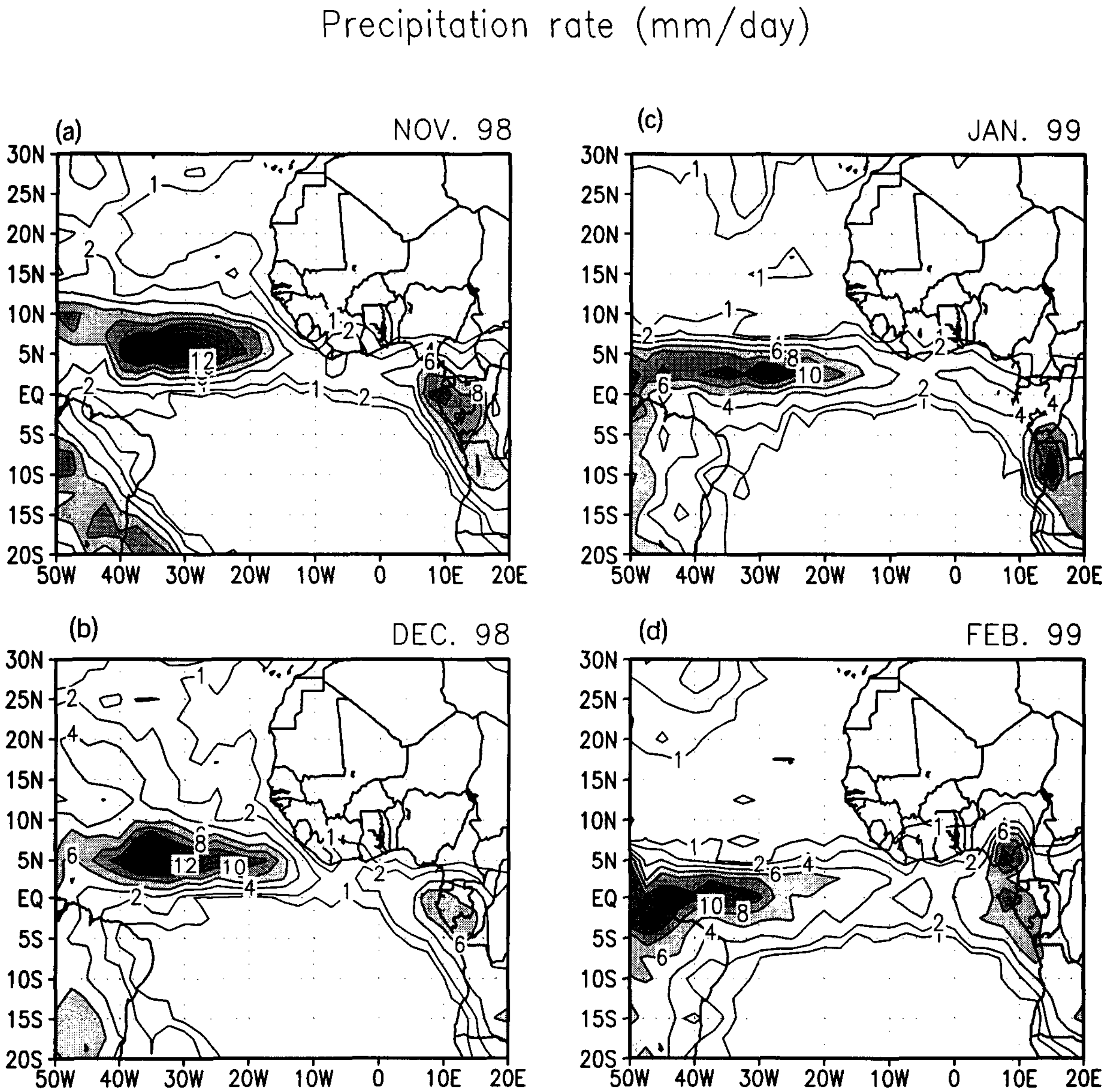

Precipitation rate (mm/day)
(a)
NOV. 98
(b)
DEC. 98
(c)
JAN. 99
(d)
FEB. 99
30N
25N
20N
15N
10N
5N
EQ
5S
10S
15S
20S
50W 40W 30W 20W 10W 0 10E 20E


Figure 8

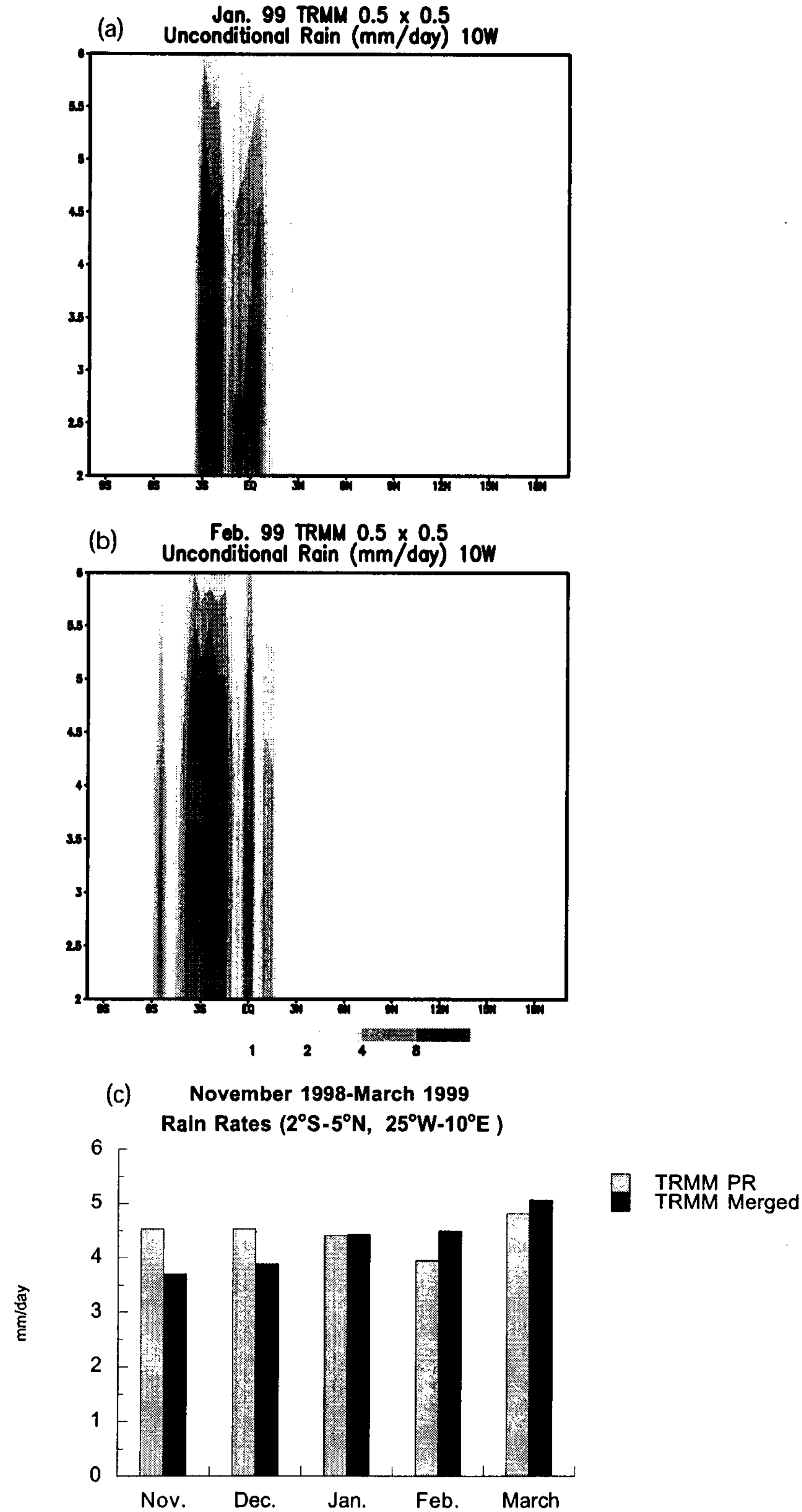
(a)
Jan. 99 TRMM 0.5 x 0.5
Unconditional Rain (mm/day) 10W
(b)
Feb. 99 TRMM 0.5 x 0.5
Unconditional Rain (mm/day) 10W
1
2
4
8
(c)
November 1998-March 1999
Rain Rates (2°S-5°N, 25°W-10°E )
mm/day
0
1
2
3
4
5
6
Nov.
Dec.
Jan.
Feb.
March
TRMM PR
TRMM Merged

Figure 9

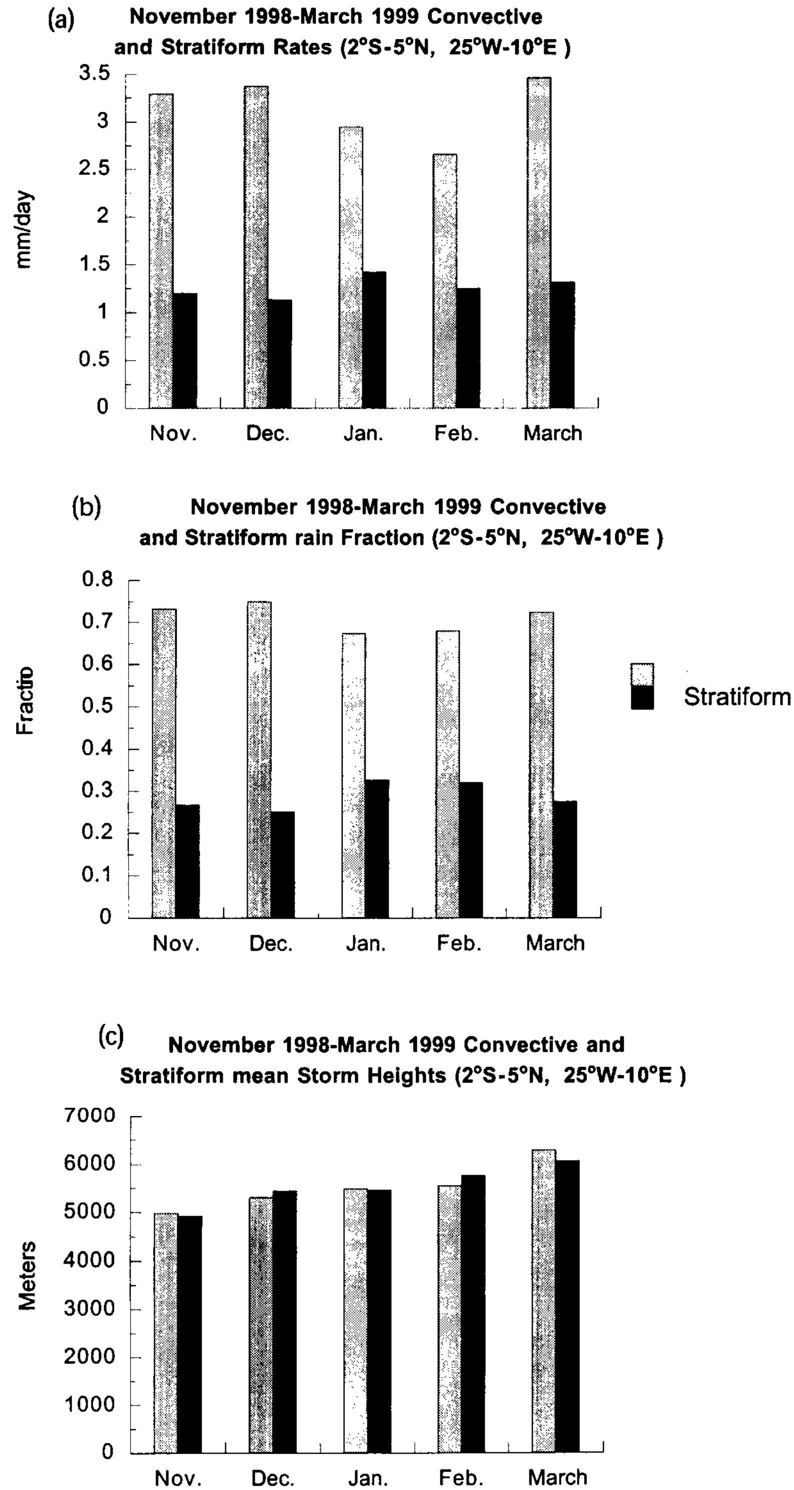
(a)
November 1998-March 1999 Convective
and Stratiform Rates (2°S-5°N, 25°W-10°E )
mm/day
3.5
3
2.5
2
1.5
1
0.5
0
Nov.
Dec.
Jan.
Feb.
March
(b)
November 1998-March 1999 Convective
and Stratiform rain Fraction (2°S-5°N, 25°W-10°E )
Fractio
0.8
0.7
0.6
0.5
0.4
0.3
0.2
0.1
0
Nov.
Dec.
Jan.
Feb.
March
Stratiform
(c)
November 1998-March 1999 Convective and
Stratiform mean Storm Heights (2°S-5°N, 25°W-10°E )
Meters
7000
6000
5000
4000
3000
2000
1000
0
Nov.
Dec.
Jan.
Feb.
March

Figure 10

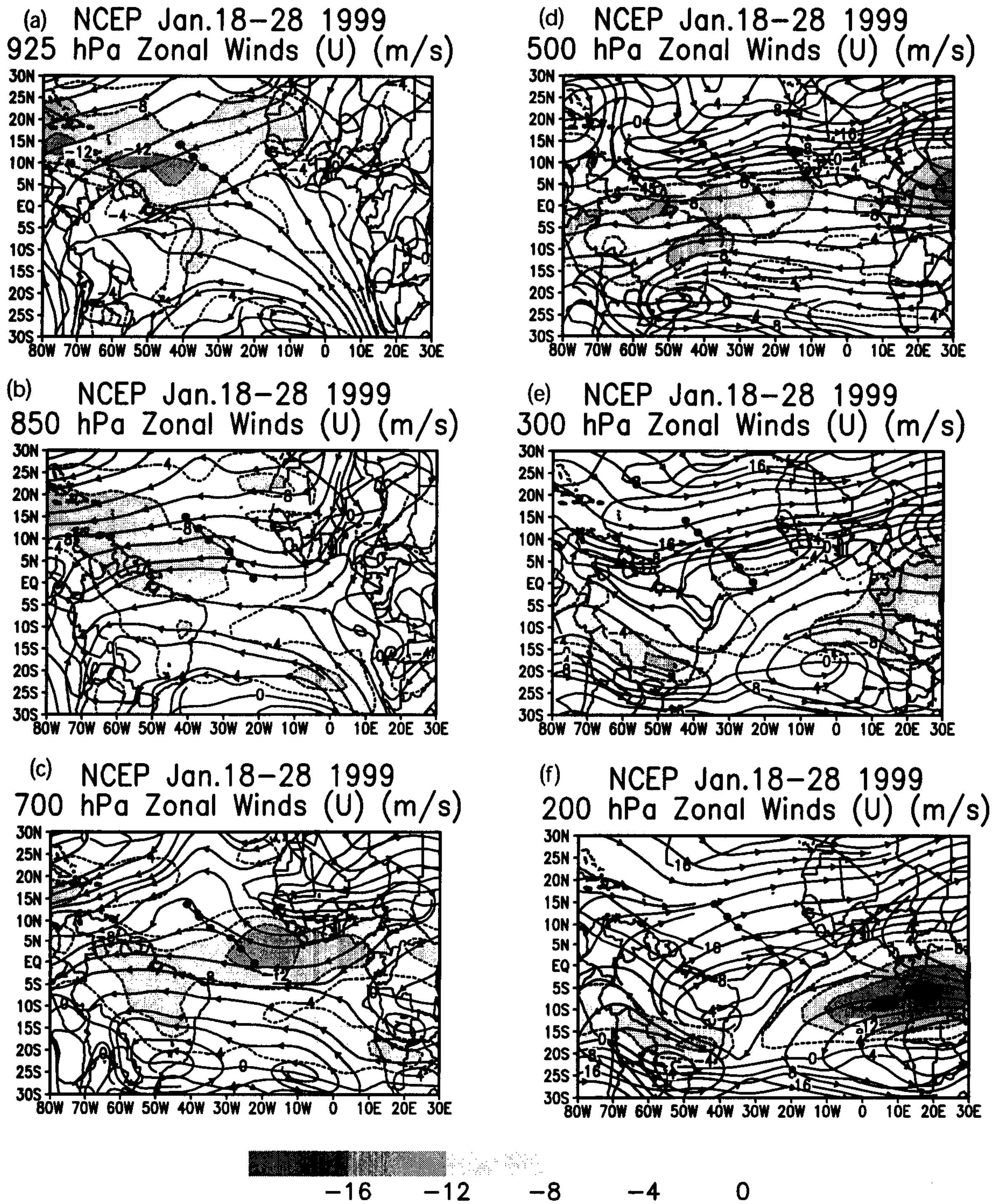
(a) NCEP Jan.18-28 1999
925 hPa Zonal Winds (U) (m/s)
(b) NCEP Jan.18-28 1999
850 hPa Zonal Winds (U) (m/s)
(c) NCEP Jan.18-28 1999
700 hPa Zonal Winds (U) (m/s)
(d) NCEP Jan.18-28 1999
500 hPa Zonal Winds (U) (m/s)
(e) NCEP Jan.18-28 1999
300 hPa Zonal Winds (U) (m/s)
(f) NCEP Jan.18-28 1999
200 hPa Zonal Winds (U) (m/s)
30N 25N 20N 15N 10N 5N EQ 5S 10S 15S 20S 25S 30S
80W 70W 60W 50W 40W 30W 20W 10W 0 10E 20E 30E
−16 −12 −8 −4 0

Figure 11

5-day Back-trajectories during Aerosols99 Cruise
Start Date: 23 January, 1999

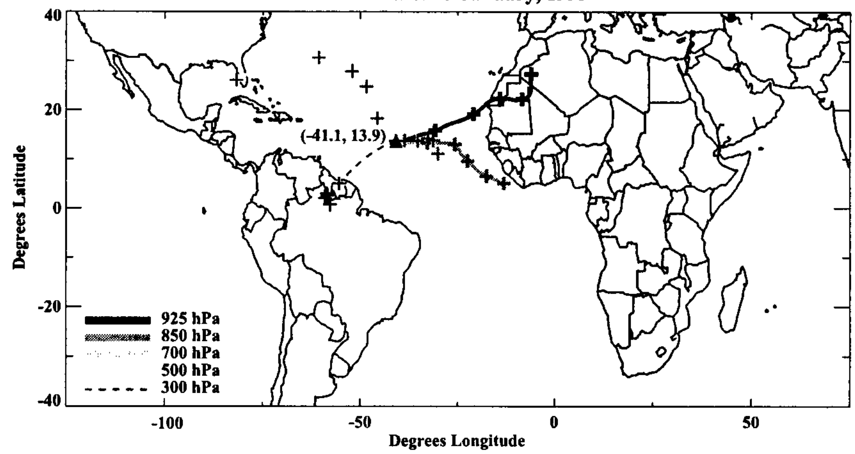


5-day Back-trajectories during Aerosols99 Cruise
Start Date: 24 January, 1999

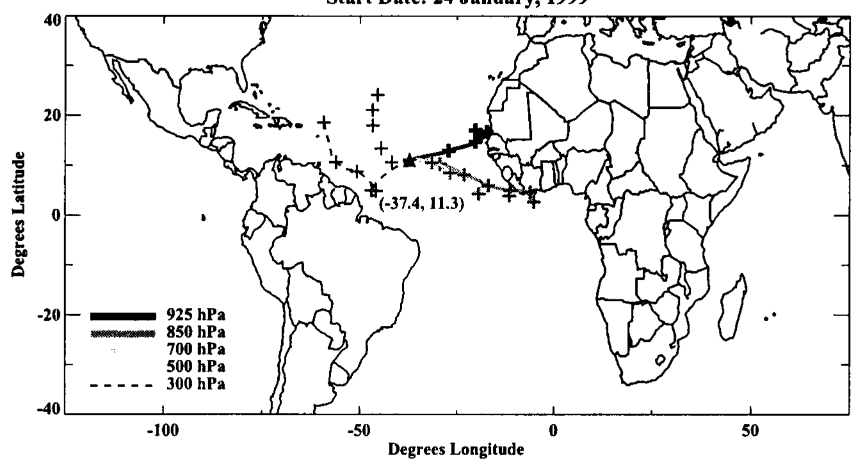


5-day Back-trajectories during Aerosols99 Cruise
Start Date: 25 January, 1999

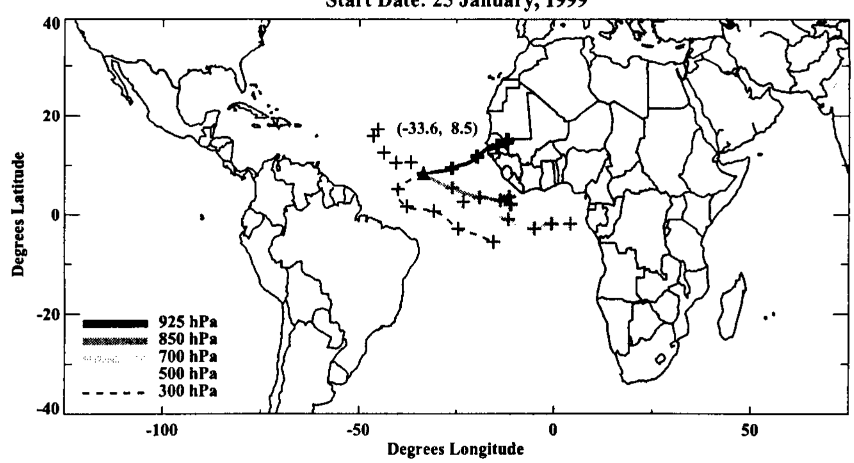


Figure 12

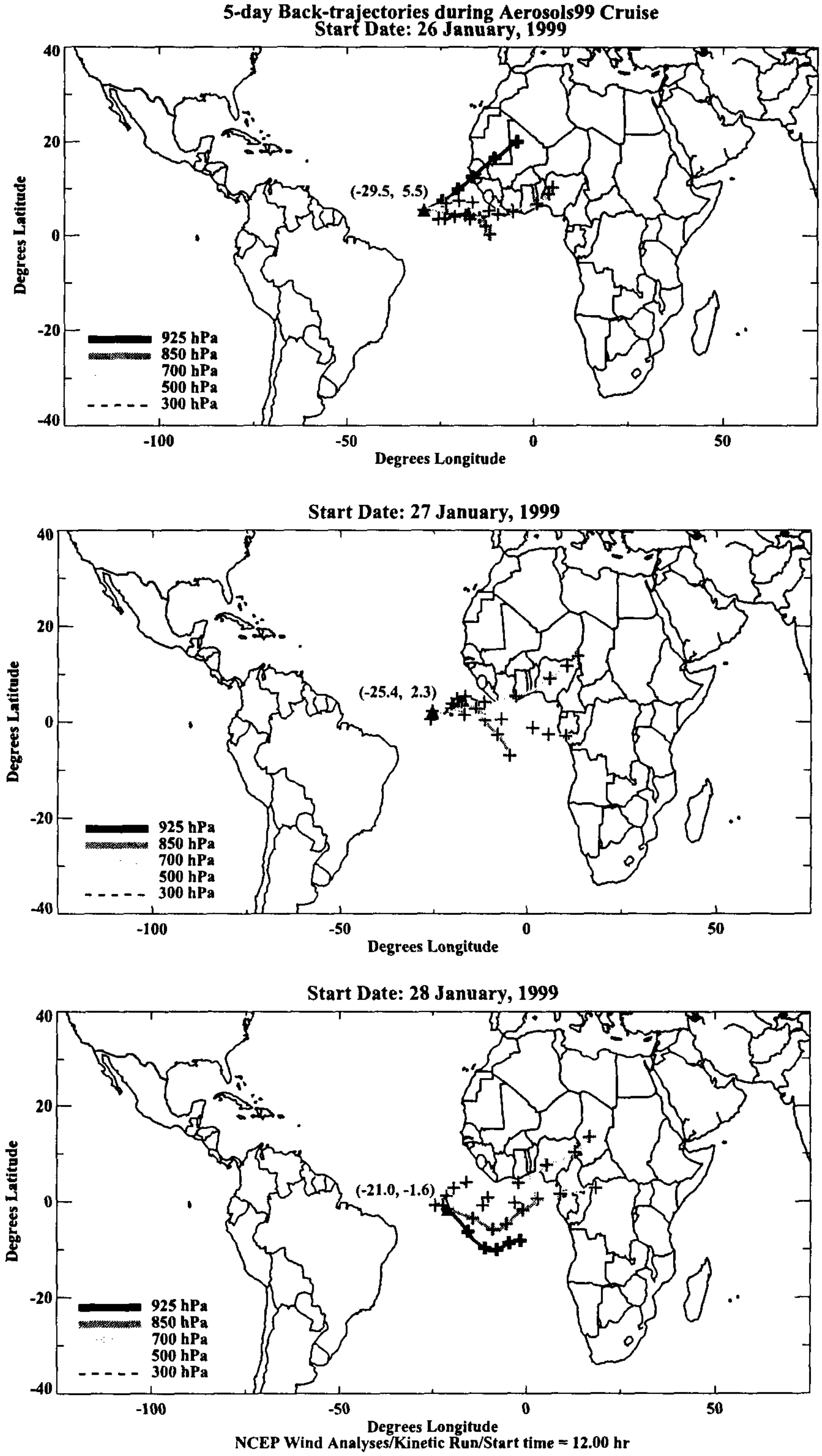


Figure 12 (Continued)

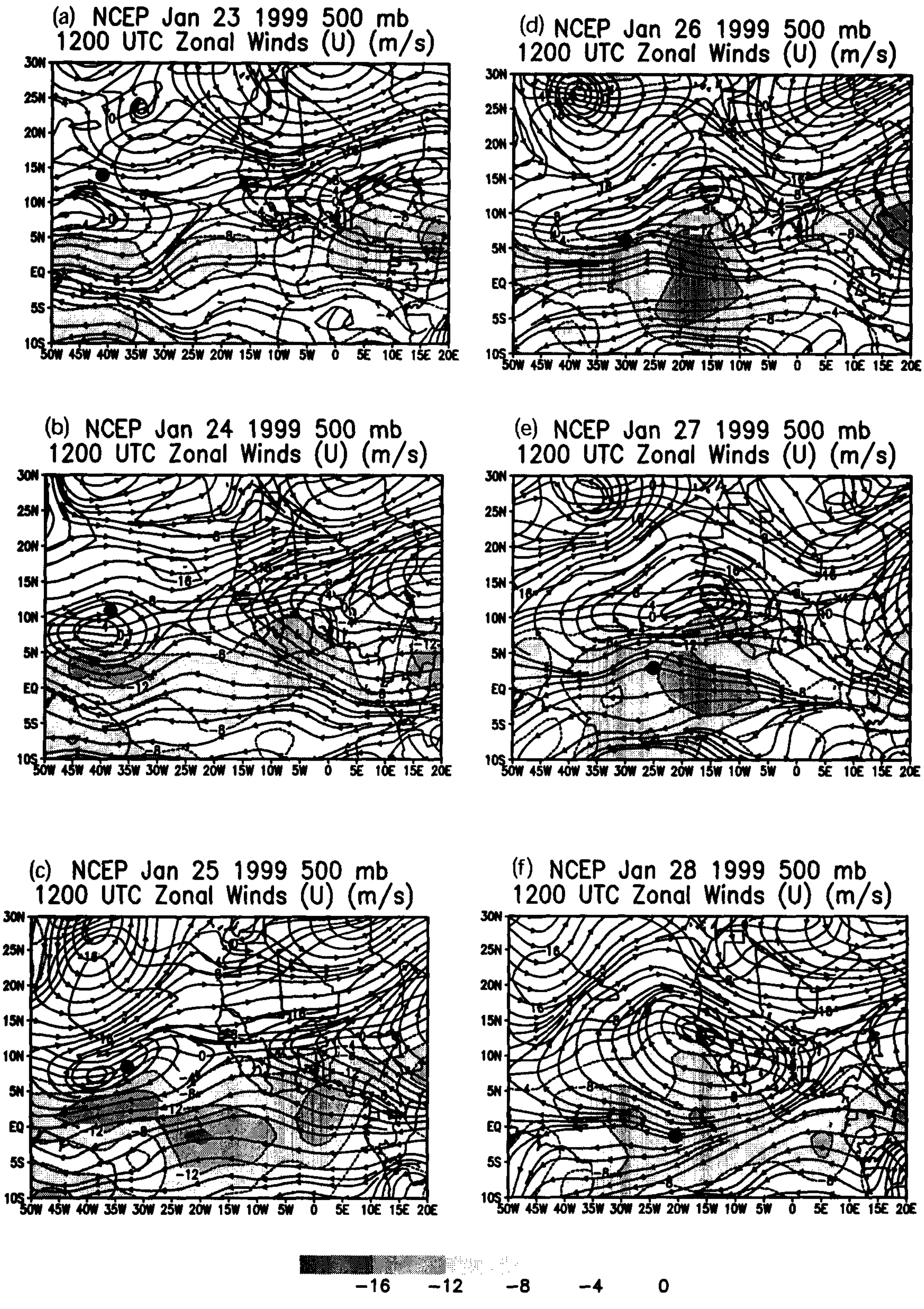
(a) NCEP Jan 23 1999 500 mb
1200 UTC Zonal Winds (U) (m/s)
(d) NCEP Jan 26 1999 500 mb
1200 UTC Zonal Winds (U) (m/s)
(b) NCEP Jan 24 1999 500 mb
1200 UTC Zonal Winds (U) (m/s)
(e) NCEP Jan 27 1999 500 mb
1200 UTC Zonal Winds (U) (m/s)
(c) NCEP Jan 25 1999 500 mb
1200 UTC Zonal Winds (U) (m/s)
(f) NCEP Jan 28 1999 500 mb
1200 UTC Zonal Winds (U) (m/s)
−16 −12 −8 −4 0

Figure 13

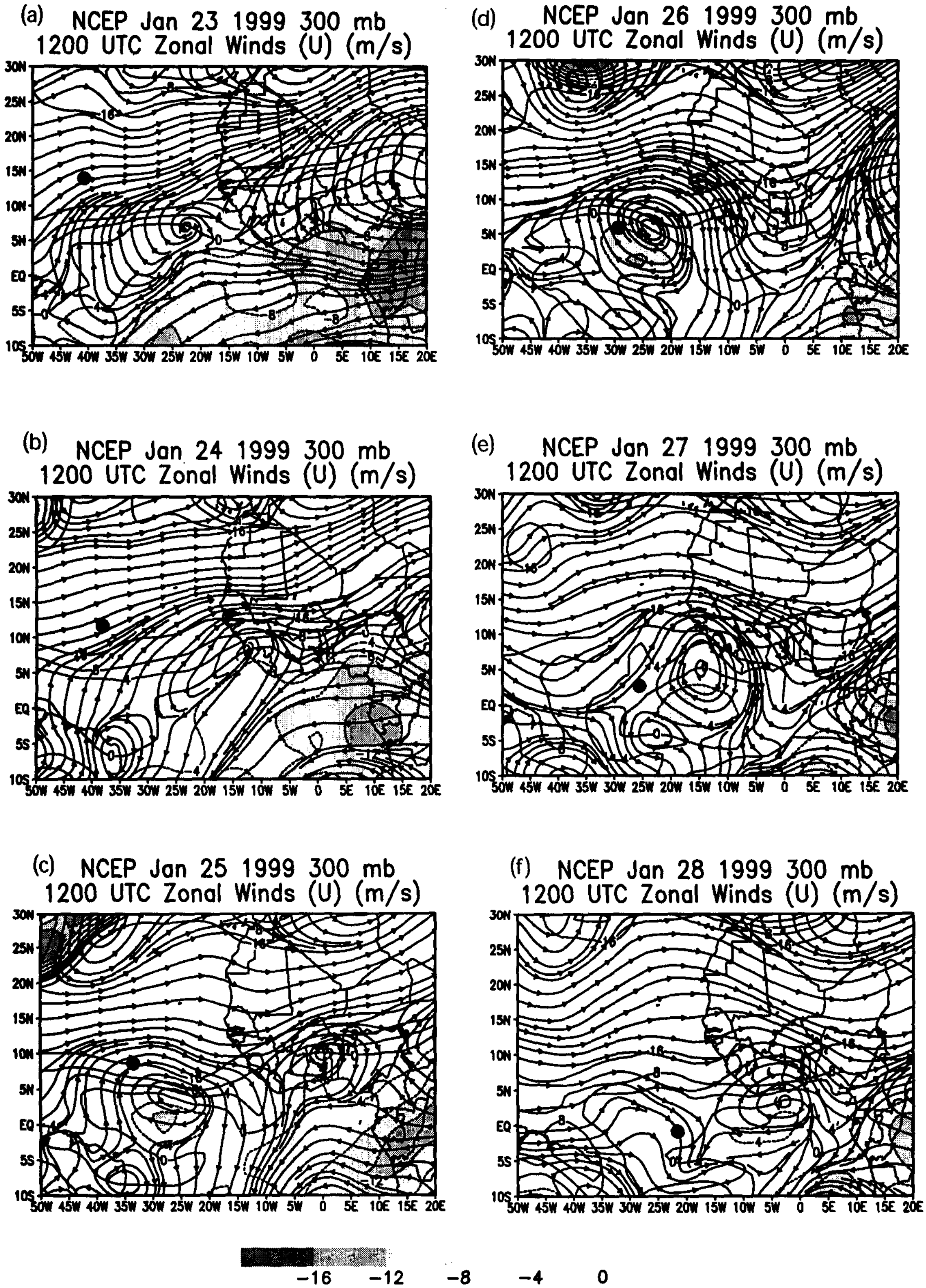
(a) NCEP Jan 23 1999 300 mb
1200 UTC Zonal Winds (U) (m/s)
(d) NCEP Jan 26 1999 300 mb
1200 UTC Zonal Winds (U) (m/s)
(b) NCEP Jan 24 1999 300 mb
1200 UTC Zonal Winds (U) (m/s)
(e) NCEP Jan 27 1999 300 mb
1200 UTC Zonal Winds (U) (m/s)
(c) NCEP Jan 25 1999 300 mb
1200 UTC Zonal Winds (U) (m/s)
(f) NCEP Jan 28 1999 300 mb
1200 UTC Zonal Winds (U) (m/s)
30N 25N 20N 15N 10N 5N EQ 5S 10S
50W 45W 40W 35W 30W 25W 20W 15W 10W 5W 0 5E 10E 15E 20E
−16 −12 −8 −4 0

Figure 14

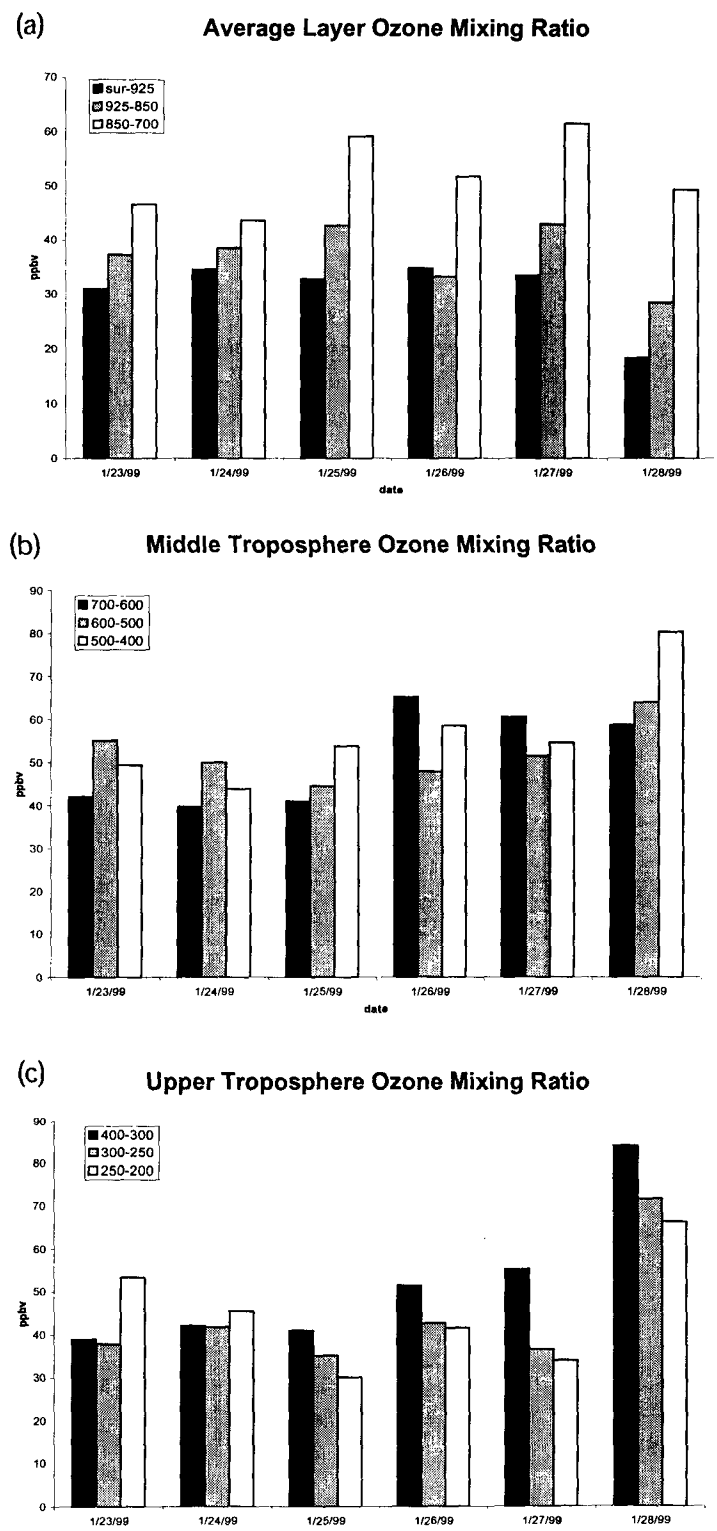
(a)
Average Layer Ozone Mixing Ratio
sur-925
925-850
850-700
ppbv
date
1/23/99
1/24/99
1/25/99
1/26/99
1/27/99
1/28/99
(b)
Middle Troposphere Ozone Mixing Ratio
700-600
600-500
500-400
ppbv
date
1/23/99
1/24/99
1/25/99
1/26/99
1/27/99
1/28/99
(c)
Upper Troposphere Ozone Mixing Ratio
400-300
300-250
250-200
ppbv
date
1/23/99
1/24/99
1/25/99
1/26/99
1/27/99
1/28/99

**Figure 15**

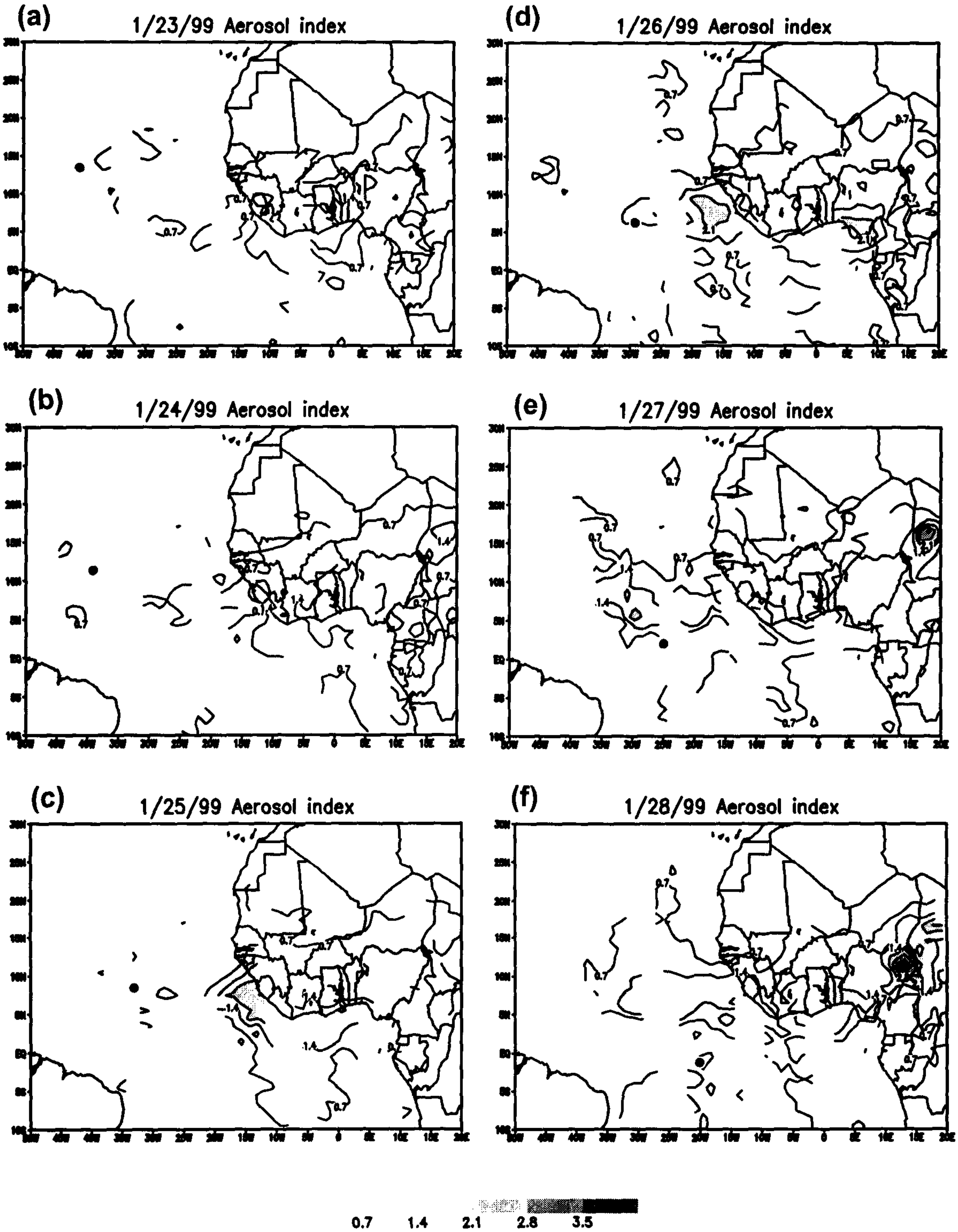
(a)
1/23/99 Aerosol index
(b)
1/24/99 Aerosol index
(c)
1/25/99 Aerosol index
(d)
1/26/99 Aerosol index
(e)
1/27/99 Aerosol index
(f)
1/28/99 Aerosol index
0.7
1.4
2.1
2.8
3.5

**Figure 16**

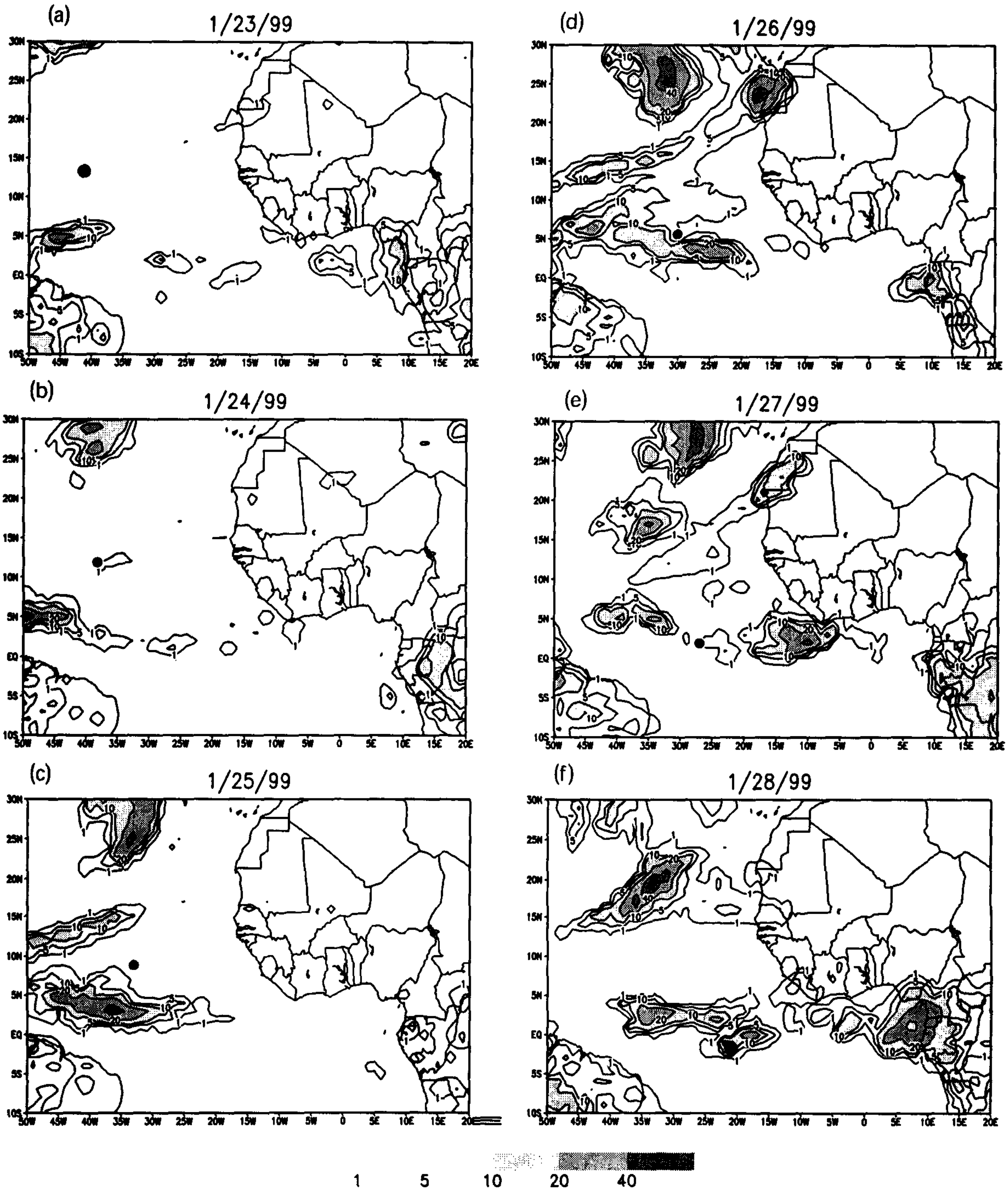


Figure 17

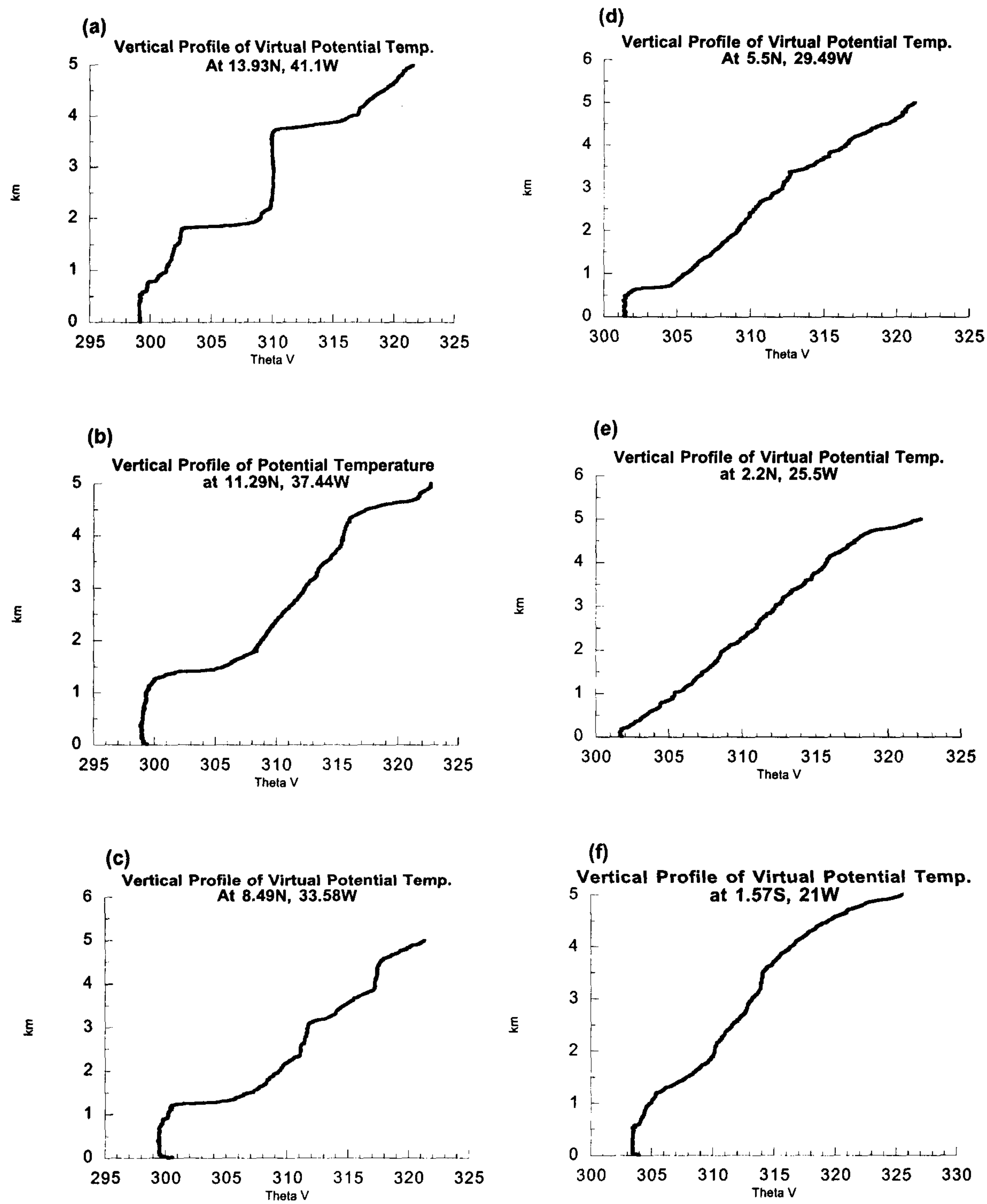
(a)
Vertical Profile of Virtual Potential Temp.
At 13.93N, 41.1W
km
Theta V
(b)
Vertical Profile of Potential Temperature
at 11.29N, 37.44W
km
Theta V
(c)
Vertical Profile of Virtual Potential Temp.
At 8.49N, 33.58W
km
Theta V
(d)
Vertical Profile of Virtual Potential Temp.
At 5.5N, 29.49W
km
Theta V
(e)
Vertical Profile of Virtual Potential Temp.
at 2.2N, 25.5W
km
Theta V
(f)
Vertical Profile of Virtual Potential Temp.
at 1.57S, 21W
km
Theta V

**Figure 18**

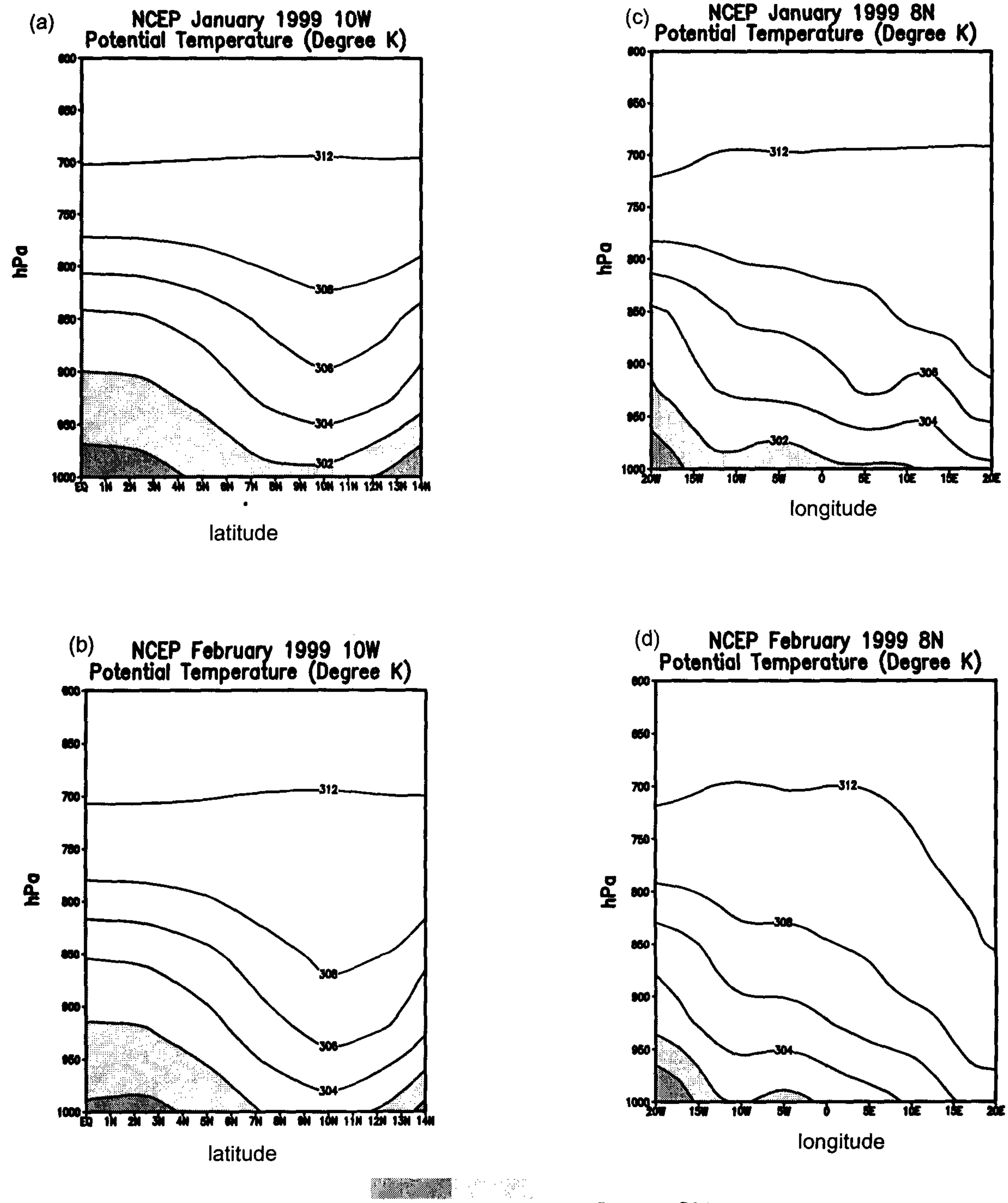
(a)
NCEP January 1999 10W
Potential Temperature (Degree K)
hPa
latitude
(c)
NCEP January 1999 8N
Potential Temperature (Degree K)
hPa
longitude
(b)
NCEP February 1999 10W
Potential Temperature (Degree K)
hPa
latitude
(d)
NCEP February 1999 8N
Potential Temperature (Degree K)
hPa
longitude
300
302
304
306

Figure 19

(a) **# of Flashes from Continental Outflow Regions**

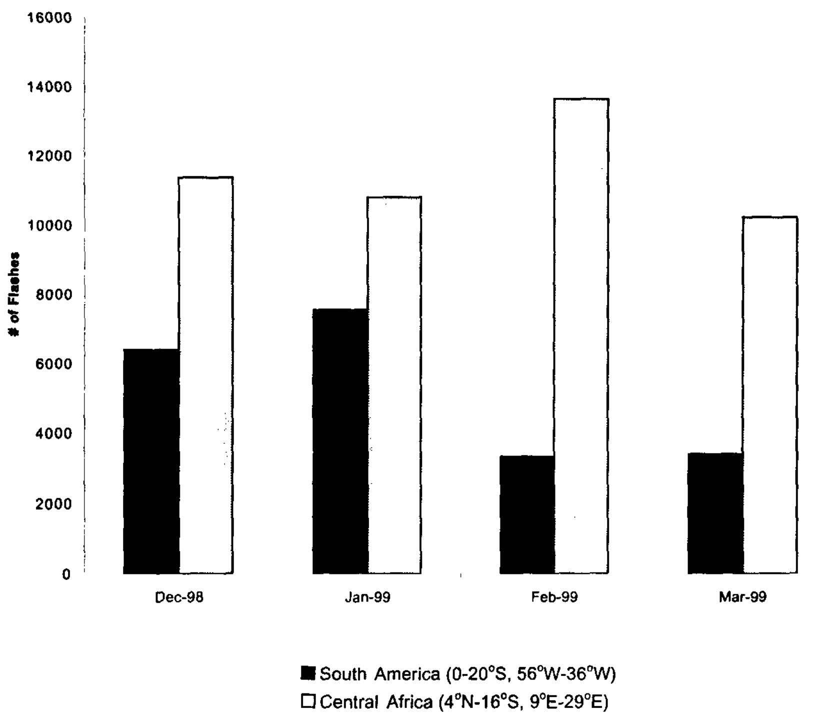


(b) **LIS daily detected Lightning Flashes from continental outflow regions**

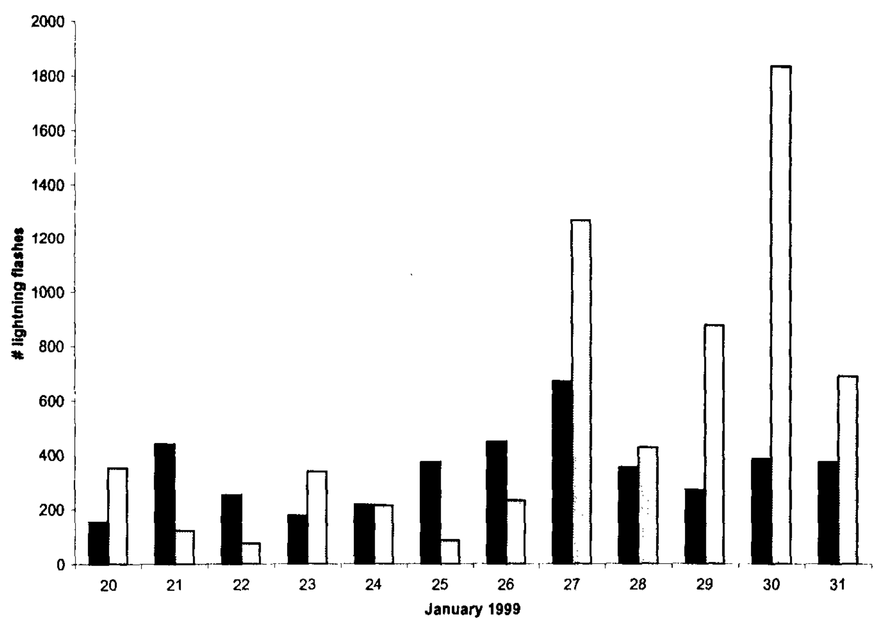


Figure 20